Yet another note on laboratory lighting

D. J. Huntley and M. R. Baril
Department of Physics, Simon Fraser University, Burnaby, B.C., V5A 1S6, Canada

(Received 25 June 2002; in final form 24 September 2002)

There have been a number of notes in Ancient TL on the subject of the lighting that should be used in the laboratory when preparing samples for luminescence dating. The most recent is that of Spooner (2000), wherein can be found an excellent detailed account of the science, and which should be consulted for earlier references. Spooner recommended the use of a low-pressure sodium lamp emitting predominantly at 2.1 eV (589 nm), with a yellow plastic filter to remove higher-energy photons, at an illumination level of 0.1 $\mu W.cm^{-2}$. Here we review the little-known earlier results of Ditlefsen (1991), and describe our own lighting which makes use of compact fluorescent bulbs and orange light-emitting diodes, which are cheaper and more convenient.

Ditlefsen (1991) reported excitation spectra, and the rates of decay of the luminescence intensity after the excitation was switched on, at excitation photon energies of 1.8-2.5 eV (670-480 nm). These data were then combined with the eye response to deduce the photon energy that would have the least effect on the sample for a given level of laboratory illumination as seen by the eye. This was done for one quartz separate and some sediment feldspars.

The result for the quartz was the redder the better; in other words as the energies of the excitation photons decreased, the probability of excitation of electrons from traps decreased faster than the eye response.

The result for feldspars was quite different. There is a clear broad optimum at a photon energy of 2.0-2.3 eV (620-540 nm), in the yellow part of the spectrum. This is shown in Fig. 1. At higher photon energies the excitation probability increases more rapidly than the eye sensitivity. At lower photon energies the excitation probability decreases less rapidly than the eye sensitivity. This result is of relevance to laboratory lighting if it is the same traps that are being emptied at the different photon energies. We have now shown that this is the case over the range 1.2 - 2.1 eV, which encompasses the resonant excitation peak at 1.4 eV used for dating, using the method described in Huntley and Ditlefsen (1994).

Our lab lighting has been designed to match the optimum at 2.1 eV. For several years we have been using compact fluorescent light bulbs that are available

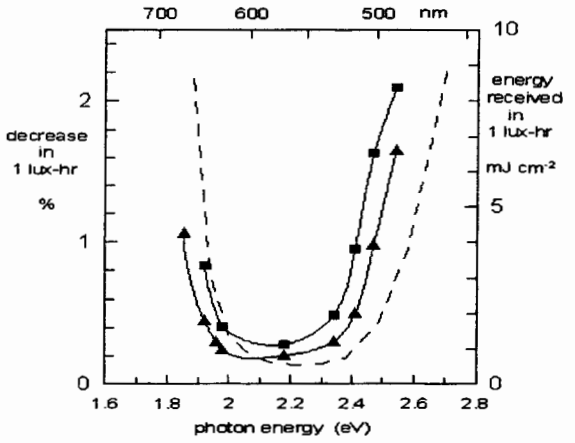

Figure 1.
The decrease in 400 nm luminescence emission during a 1 lux-hr exposure to photons of the energy shown. Solid triangles are for 100-200 μm K-feldspars separated from Riso sample R908002 (Tirstrup); solid squares are for 4-11 μm grains from loess from Karamaidan, Tadzhikistan. Solid lines are spline fits to the data. The dashed line shows the incident energy during a 1 lux-hr exposure. The data are from Ditlefsen (1991, Ch 4). (1 lux = 1 lumen cm^{-2}).

in hardware stores. The particular kind we use is an 18 W Philips, and has a complete plastic cover which is roughly a 6 cm diameter by 10 cm long cylinder. These are relatively inexpensive, and are convenient because they screw into ordinary ceiling or desk-lamp light sockets. They emit an insignificant amount of infrared light, as is necessary when preparing feldspars. They do, however, require a filter to eliminate the high energy photons. For this we use an orange filter designed to wrap around the long fluorescent light tubes, the same type as traditionally used in thermoluminescence work. A piece of this is 13.3 x 119 cm. From one of these we cut a piece about 4 x 119 cm, wrap it around the middle of the compact fluorescent bulb, and use black electrician's tape to hold it in place and cover the rest of the bulb. The only light then emitted is from a 0.8 cm wide strip around the middle of the bulb.

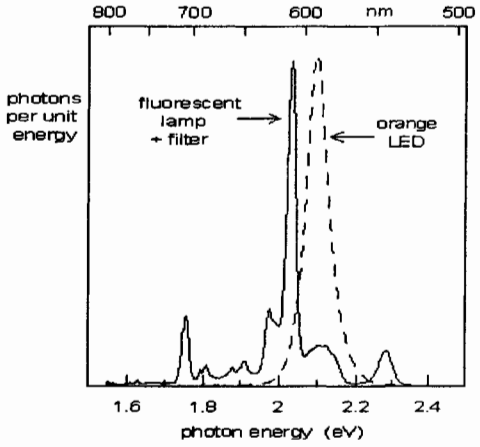

Figure 2.
Emission spectra for a Philips 18 W compact fluorescent lamp fitted with a filter as described in the text, and a Photon Micro-Light® orange LED as sold.

The spectrum of the light emitted by a bulb outfitted with such a filter is shown in Fig.2.

We have tested its use on feldspars separated from a Tertiary sample (CBSS), and found the luminescence emitted under 1.4 eV excitation to be decreased by 0.07 % per hour of exposure of the grains when the light was in a ceiling light socket. In fact most of the light was arriving at the sample after reflection from the walls of the room. The light intensity was 0.2 μW cm^{-2}. This light intensity is adequate for most work, but an increase of an order of magnitude could be tolerated for short periods.

For some years also we have used ordinary pocket flashlights in which we have replaced the bulbs by an orange light-emitting diode and a suitable resistor. These are very convenient for hand use. One has to be careful since some such LED's emit some light at higher photon energies and it can be necessary to add an orange filter. There has recently appeared on the market some very convenient flashlights using orange LED's (and other colours). These are made by Photon[a], cost about Can$12, are designed to be attached to a key ring or zipper pull, and are available at outdoor stores. A spectrum of one is shown in Fig.2. We have tested exposure of feldspars separated from a tertiary sandstone (sample CBSS) to light from one and found the effect to be ca 0.5 ± 0.1 % per minute of direct illumination at a distance of 20 cm, the intensity being 100 μW.cm^{-2}. This is much brighter than one needs in practice; it does, however, permit one to view a sample in a bright light for a few seconds. This LED is also very convenient for looking in dark cupboards, drawers etc, and I expect to use it in the field when sampling in the dark

The data of Ditlefsen, Spooner and those presented here all show that an exposure of 1 lux-hour, which at 2.1 eV corresponds to 0.1 μW cm^{-2} for about 2 hours, causes a reduction in the 1.4 eV-stimulated luminescence under 1 %.

[a] Photon Micro-Light®, L.R.I., P.O.Box 58, Blachley, Oregon, 97412-9718, U.S.A.

References

Ditlefsen, C. (1991). Luminescence dating of Danish Quaternary sediments. Ph.D. thesis, University of Aarhus, Denmark.

Huntley, D.J. and Ditlefsen, C. (1994). Optical excitation of trapped charges in quartz, potassium feldspars and mixed silicates: the dependence on photon energy. *Radiation Measurements* **23**, 675-682.

Spooner, N.A., Questiaux, D.G. and Aitken, M.J. (2000). The use of sodium lamps for low-intensity laboratory safelighting for optical dating. *Ancient TL* **18**, No.2, 45-49.

Reviewer

J. Prescott

Detection of far-red IRSL from loess

Zhong-Ping Lai[1], Lee Arnold[1], Stephen Stokes[1], Richard Bailey[1], and Morteza Fattahi[1,2]
1. Oxford Luminescence Research Group, School of Geography and the Environment, University of Oxford, Mansfield Road, Oxford, OX1 3TB, UK
2. Institute of Geophysics, University of Tehran, Iran
Corresponding author. E-mail: zhongping.lai@geog.ox.ac.uk. Fax: +44-1865-271929.

(Received 7 October 2002; in final form 20 October 2002)

Abstract: *It has recently been proposed that it may be possible to extend the age range of luminescence dating of loess using the far-red (λ=665-740nm) emission from feldspar, as it is thought not to exhibit anomalous fading. Studies on red luminescence have been hindered due to technical difficulties in suppression of background and other factors. Recently modifications to apparatus (esp. photo-multiplier plus filter combinations) have been reported demonstrating that red IRSL (λ=590-700nm) may be observed from coarse-grained feldspar (Fattahi and Stokes, 2002a). However, this modified system was not able to detect far-red IRSL (λ=665-740nm) from old (>800ka) Chinese loess. In this short note we describe further modifications to the system which have successfully enhanced the far-red IRSL signal, and at the same time reduced background signal levels. As a result, routine measurements of far-red IRSL from loess are possible.*

Introduction

The luminescence dating of feldspar using UV-blue emissions has been hindered by the ubiquitous presence of anomalous fading and associated age underestimation (e.g. Lamothe and Auclair, 1999; Huntley and Lamothe, 2001). Red TL (λ>600nm) of feldspar has been demonstrated not to exhibit anomalous fading (Zink and Visocekas, 1997). The work of Zink and Visocekas (1997) was, however, focussed on a relatively small number of samples and exploited relatively low temperature (<370°C) red TL. A logical extension of their investigations is to study red IRSL from feldspar (Fattahi, 2001).

Recently, Fattahi and Stokes (2002a) have successfully demonstrated that it is possible to detect red IRSL (λ=590-700nm) from coarse grain potassium-rich feldspar by careful selection of novel photo-multiplier (PMT) and filter combinations. In further testing we have found that their system is not able to observe far-red IRSL (λ>665nm) from loess sample as old as 800 ka (expected D_e c. >3,000Gy). Here we describe further developments to the detection system that allow far-red IRSL from loess with doses as low as 50Gy to be measured.

Selection of detection window

There are a variety of luminescence emissions of feldspar from 280 to 800nm (Krbetschek et al., 1997). The conventionally used UV/blue emissions suffer from anomalous fading (e.g. Lamothe and Auclair, 1999). The pioneering work by Zink and Visocekas (1997) has shown that while blue TL of volcanic feldspars (λ<600nm) suffers severely from anomalous fading, red TL (λ>600nm) from the same samples does not fade anomalously. Fattahi and Stokes (2002b) reported that orange-red IRSL (λ=590-700nm) from potassium feldspar derived from sediments exhibited anomalous fading, but at a level much lower than blue IRSL, and that far-red IRSL (λ=665-700nm) showed no fading. It seems that the further toward IR we are able to detect red IRSL, the more stable a signal we observe. We interpret this as a reflection of a progressive reduction of the influence of the broad yellow-orange (~570nm) emission centre which has previously been recognized to exhibit fading (e.g. Fattahi and Stokes, 2002b).

It has been demonstrated that loess has a strong far-red emission (λ=665-740nm) in both natural and laboratory irradiated polymineral samples (Krbetschek et al., 1997; Lai et al., 2002). Moreover, far-red IRSL is highly reproducible and amendable to Single Aliquot Regenerative (SAR) techniques (Fattahi and Stokes, 2002c; Lai et al., 2002; Arnold et al., 2002). As a result, we here further focus on the wavelength band of 665-740nm (far-red IRSL) as the optimum detection window (filter combination is Schott RG 665 + Omega 740 SP, Fig 1). The difficulty in detecting far-red IRSL at this wavelength is the suppression of high background related to the close proximity of the IR stimulation source (λ=830 ± 5nm).

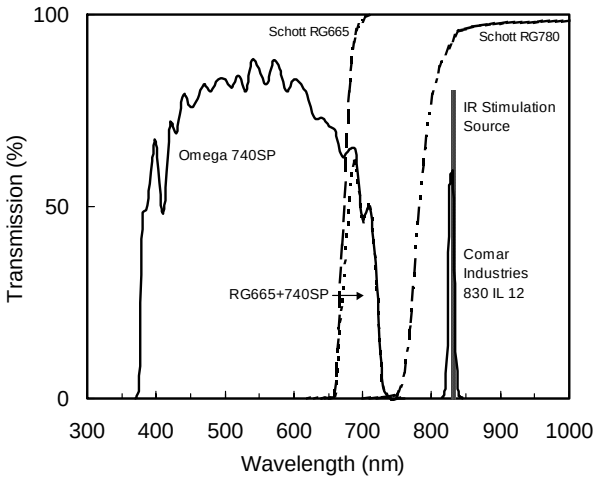

Figure 1.
Detection and stimulation windows.

The sources of background

There are two main contributions to background----dark counts from the photo-multiplier tube (PMT), and reflected light from IR stimulation (Fattahi, 2001). The dark count of the extended range PMTs used for red emission studies is constant and can be reduced by an order of magnitude down to about 200 c/s by cooling the PMTs down to ~-15^{o}C (Fattahi and Stokes, 2002a). The remaining primary contribution to the background signal is from reflected incident IR stimulation photons and related emissions, due to the close positioning of detection (665-740nm) and stimulation (830 ± 5 nm) windows.

A suitable PMT should be chosen for the purpose of detecting far-red IRSL, and at the same time reducing the background from IR stimulation. There is no ideal PMT with high quantum efficiency (QE) at far-red emission and 0% QE at other wavelengths (see Fig 1 in Fattahi and Stokes, 2002a). While the conventionally used EMI bialkaline 9635 PMT (blue) is highly sensitive to UV/blue emission and has also been used for quartz orange-red TL (c. 600-620nm) detection (e.g. Miallier et al., 1991), it has no QE at wavelengths greater than 650nm, making it unsuitable for far-red emission detection. The EMI bialkline S20 9650 (red) PMT has high QE (5%) at 700nm. However, it has a QE of 1% at 830nm (the stimulation peak), which typically results in high background (~>10^{6}c/s). The EMI Biakaline D716A S11 (green) PMT has a QE of 0.1% at 700nm and a QE of less than 0.01% at 830nm, making it acceptable for far-red IRSL detection (Fattahi, 2001; Stokes and Fattahi, 2002).

In efforts to detect far-red IRSL from fluvial coarse grain feldspar, Fattahi and Stokes (2002a) have made the following adjustment to the standard Risø TA-15a TL/OSL system (Bøtter-Jensen, 1997), which incorporates an IR laser diode (400mW, 830±5nm) and a ^{90}Sr/^{90}Y beta radioactive source:

1. An extended EMI D716A S11 (green) PMT was used.
2. An S 600 Photocool Thermoelectric Refrigerated Chamber was fitted to cool the PMT (c. ~ - 20^{o}C). This reduces PMT dark counts by an order of magnitude, down to c. 200 c/s.
3. The far-red IRSL was detected using a combination of Schott RG665 + 2*Corion FR400S + Schott BG39 filters, with an estimated detection band of 665-700nm (Fattahi and Stokes, 2002c).

The above modifications make it possible to detect far-red IRSL from fluvial coarse grain feldspar (bright sample), with background at a level of below 500 c/s (Fattahi, 2001). However, using this configuration it has not been able to detect far-red IRSL from loess. Figure 2 shows IR exposure decay curves measured using this configuration. While coarse grain feldspar (sample 15/1, 90-120μm, age c. 23.2 ± 1.8ka) gave a relatively high signal to noise ratio (3.64), no signal was distinguishable above background for a natural loess sample (age c. 800ka, D_e > 3,000Gy, grain size of 4-11 μm). By increasing the grain size to 11-78μm it is possible to detect a small red emission IRSL signal from this sample (initial signal = 400 c/s above background, ~0.13 c/Gy), but at a level which is not suitable for routine dating application.

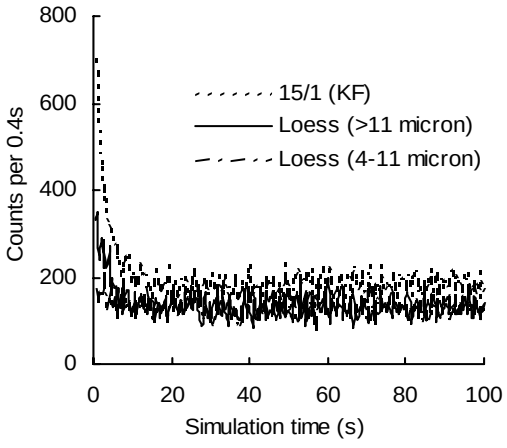

Figure 2.
Far-red IRSL signal level of loess and fluvial coarse grain feldspar using the detection system development by Fattahi and Stokes (2002a). IRSL was measured at 150^{o}C.

No.	**S11 PMT (Green)** **Filter combination**	**Sample: 15/1** **S (Signal)**	**N (Noise)**	**S/N**	**S-N (Net signal)**
1	740SP+RG665	301,158	188,157	1.6	113,002
2	FR400S+RG665	346,106	281,803	1.2	64,303
3	2*FR400S+RG665	37,542	6,950	5.4	30,592
4	2*FR400S+740SP+RG665	25,954	4,489	5.8	21,465
5	FR400S+740SP+RG665	61,418	20,178	3.0	41,241
6	BG39+2*FR400S+RG665	3,677	815	4.5	2,862
7	BG39+FR400S+RG665	7,598	1,862	4.1	5,737
8	BG39+740SP+FR400S+RG665	6,668	2,459	2.7	4,208
9	BG39+740SP+RG665	28,499	19,549	1.5	8,950
10	SWP685+2*FR400S+RG665	5,527	1,097	5.0	4,430
11	SWP685+FR400S+RG665	15,244	6,018	2.5	9,227
12	SWP685+740SP+FR400S+RG665	8,952	1,903	4.7	7,048
13	SWP685+740SP+RG665	19,697	4,630	4.3	15,067
14	SWP685+RG665	7,579,798	7,077,072	1.1	502,727
	S20 PMT (Red) **Filter combination**	**Sample: 1023/2** **S (Signal)**	**N (Noise)**	**S/N**	**S-N (Net signal)**
15	2*FR400S+RG665	716,193	655,953	1.09	60,240
16	2*FR400S+RG665+SWP685	36,918	34,904	1.06	2,013
17	2*FR400S+RG665+SWP685+BG39	36,354	35,175	1.03	1,179
18	2*FR400S+RG665+SWP685+HA3	250,189	234,695	1.07	15,494
19	2*FR400S+RG665+SWP685+740SP	162,993	152,562	1.07	10,431
20	2*FR400S+RG665+740SP	184,213	172,559	1.07	11,653
21	2*FR400S+RG665+BG39	343,481	324,731	1.06	18,750

Table 1.

Results of filter combination and PMT tests

Bright potassium-rich samples (90-120μm) 15/1 (age c. 22.2 ± 1.8ka) and 1023/2 (age c. 86 ± 6ka) (Colls, 1999) were used. It has been demonstrated that far-red IRSL from these samples exhibit no sensitivity change (Fattahi, 2001). Sample were mounted on stainless steel discs, bleached and administered a dose of 110Gy. IRSL was measured at 30^{o}C for 100s after preheat at 250^{o}C for 10s, and the IR diode power is kept at 90%. IRSL was then re-measured to obtain a background. The far-red IRSL signal was integrated over the first 1 s. The thickness of filters used: 740SP 4mm; FR400S 8mm; BG39 1mm; others 3mm.

Tests of additional signal pass filters

The purpose of using IR-cut filters in front of a photo-multiplier tube is to block the reflected light from IR laser diode. The IR-cut filters available are Schott BG 39, Omega 740 SP, Corion FR 400S, and Delta SWP BL 685 (Fig 3). Fattahi and Stokes (2002a) presented data for a variety of IR-cut filter combinations. However, most of their testing focused on a detection band of 590-700nm. This orange-red region feldspar emission has been shown to exhibit anomalous fading (Fattahi and Stokes, 2002b) due to possible influence of a 570nm emission centre. We have tested additionally filter combinations with far-red (λ=665-740nm) transmission, together with both S11 (Green) and S20 (red) PMTs (Table 1).

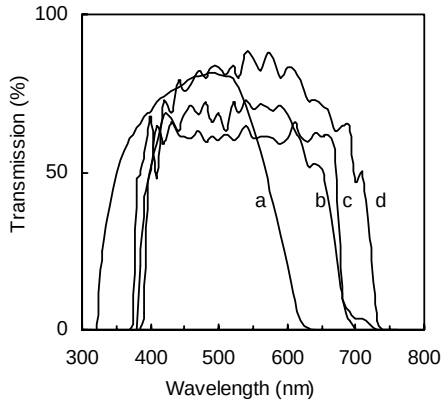

Figure 3.
Transmission characteristics of IR-cut filters (redrawn from Fattahi and Stokes 2002a). (a) Schott BG 39; (b) Corion FR 400S; (c) Delta SWP BL 685; (d) Omega 740 SP.

The S20 (red) PMT was found to result in high backgrounds using all filter combinations and yields poor signal to noise ratios. For the S11 (green) PMT, the filter combination of 2*FR400S + 740SP + RG665 gives the highest signal to noise ratio (5.8), and produces high net signal (21 kc/s) with a background level of 4.5 kc/s. The filter combination of 2*FR400S + RG665 gives a signal to noise ratio of 5.4, and produces higher net signal (30 kc/s) with a background level of 6.9 kc/s. The combination of BG39 + 2*FR400S + RG665 has the lowest background level (815 c/s) with a signal to noise ratio of 4.5, but produces very low net signal (2.9 kc/s). The BG39 is not ideal for far-red IRSL detection, as the transmission at 700nm is less than 1%. As a result, the combination of RG665 + BG39 focuses the band of below 700nm (665-700nm) which has possibly more influence from the 570nm emission peak. For bright, coarse-grained potassium-rich feldspar samples, the combinations of 2*FR400S+RG665 and 2*FR400S + 740SP + RG665 are suitable for far-red IRSL detection (λ=665-700nm), combined with a cooled S11 (green) PMT.

The combination of 740SP and RG665 filters results in a very high net signal (113 kc/s), but also gives a high background (188 kc/s). This high signal pass combination would be suitable for loess sample, if the background could be reduced. There are two possible means by which the background derived from the IR stimulation source might be reduced: (1) Shifting the wavelength of the stimulation source to a longer value, while remains within the feldspar resonance; (2) Filtering the existing IR source (λ=830 ± 5m) in order to remove or reduce any associated short wavelength emissions. In the absence of alternative IR sources at our disposal, we have investigated filtering of the existing source.

Long-pass and interference filtering of the IR stimulation sources

To maximize far-red IRSL emission the detection window should closely match that of the far-red emission centre (c. λ=720-740nm, Krbetschek et al., 1997). Our attempts to exploit this wave band have consistently resulted in high backgrounds (c. 250 kc/s with IR laser diode power at 90%) which we attribute to reflected and scattered Raman and other emissions from the IR source (Fig 4a,b).

We have tested a number of filter combinations to restrict short wavelength (i.e. λ<c. 780nm) transmission from the IR source. Firstly, various thickness (3-12mm) of Schott RG780 (Fig 1) long pass filter was attached to the front face of the IR laser diode. The IR laser stimulation source was then switched on at a constant power and the reflected IR from a blank stainless steel disc was detected. We found that 6mm of RG 780 was capable of reducing the background down to c. 124 kc/s (Fig 4c). Addition of further RG 780 filters was problematic given the limited amount of space available within the Risø diode array housing. We additionally tested an interference filter to try to both reduce background and minimise the total thickness of filters. For this purpose we used a Comar Industries 830IL12 filter (transmission 830 ± 12nm, Fig 1). The filter was tested alone, and in combination with 6mm RG780. We found that the optimum background (c. 4.2 kc/s) was achieved via a combination of both filters (Fig 4d).

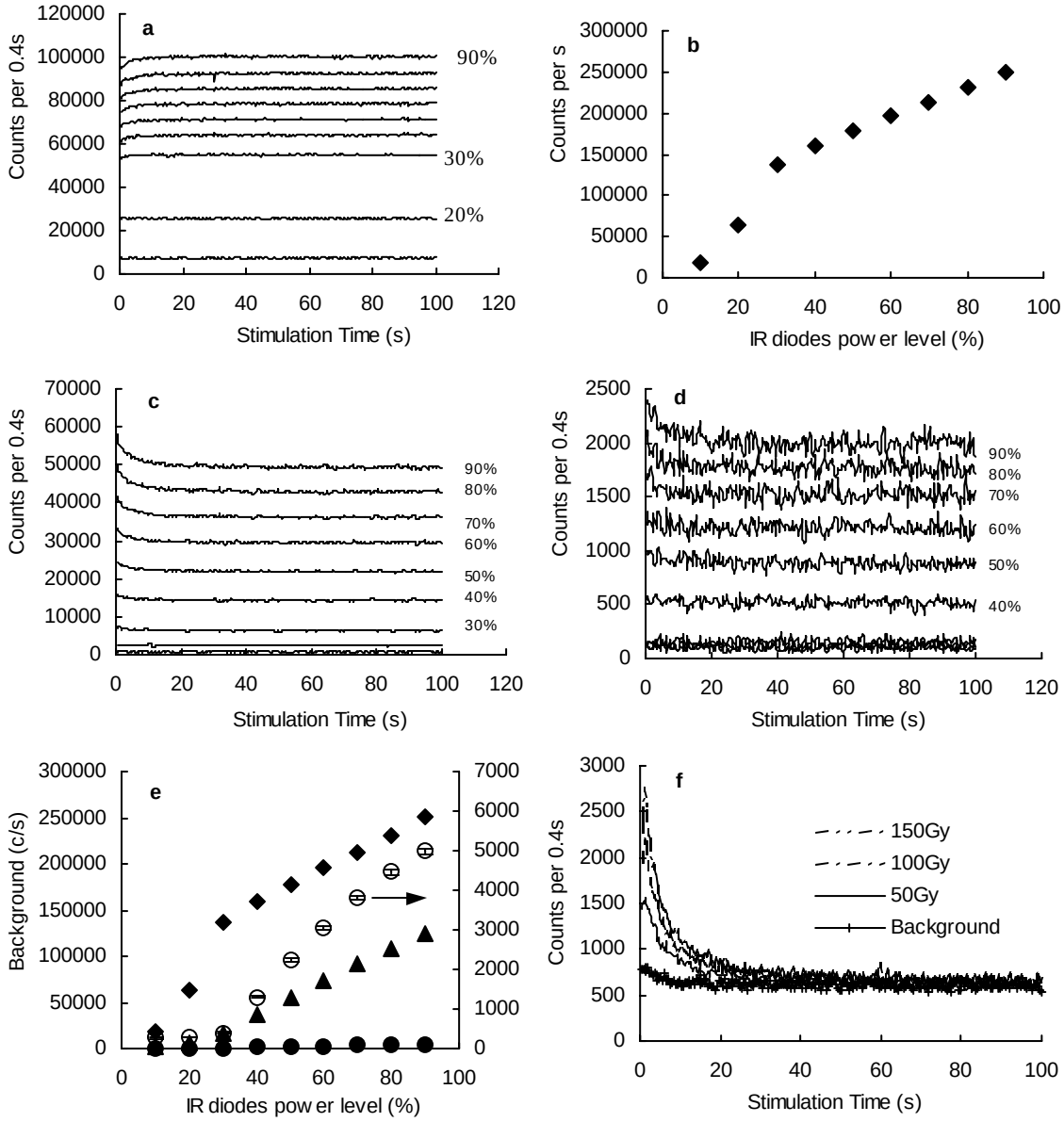

Figure 4.

Background reduction for far-red IRSL detection via additional filtering of IR light source. IRSL was measured at 30°C for 100s on a blank stainless steel disc except in (f). Detection filter combination is RG665 + 740SP. PMT is S11 (green). (a) Background vs stimulation time for a range of IR laser diode power levels; (b) Background counts vs IR diode power for (a); (c) Background vs stimulation time for a filtered IR diode source (filter is 6mm RG780); (d) Background vs stimulation time for a filtered IR diode source (filter combination is 6mm RG780 + 830IL12); (e) Comparison of background levels of filter combinations in front of IR diode. Full circle: 6mm RG780 and 830IL12; full triangle: 6mm RG780; full diamond: none; Empty circle (right Y-axis) is the enlargement of full circle for clarity. All error bars are smaller than the symbols. (f) IR exposure decay curves of far-red IRSL from laboratory irradiated loess, using the configuration in (d). IRSL was measured at 30°C for 100s after preheat at 250°C for 1min. Sample is L9/M, grain size 11-78μm, polymineral.

Discussions

We have extended the investigations of Fattahi (2001) by exploiting the combined result of filtering both the incident (IR) and reflected samples-derived luminescence. By filtering the IR laser diode with both glass and interference filters we successfully reduced the background to an acceptable level, and at the same time by exploiting Omega 740SP and Schott RG665 filters in front of the S11 (green) PMT, maximized the signal from the sample. Figure 4f shows measurements of dose response of far-red IRSL from loess using the present PMT + filter configurations. A 50Gy dose generated a net initial signal level of 1.8 kc/s with a signal to noise ratio of 2.0 and a background level of 1.9 kc/s. The 150Gy has a net initial signal level of 4.3 kc/s with a signal to noise ratio of 4.0.

Conclusions

For routine analysis of far-red IRSL from loess we recommend the use of an EMI biakaline D716A (green) PMT (S11). The EMI S20 9650 (red) PMT is less suitable due to the difficulties in suppression of background. The filter combination of Omega 740SP + Schott RG665 is chosen for the detection of far-red IRSL (λ=665-740nm) from loess. This combination produces high net signal from sample, but result in high background, and low signal to noise ratio. The background can be reduced to an acceptable level (<2,000 c/s) by attaching additional filters (a 830IL12 plus 6mm of RG780) in front of IR laser diode. The system developments described here enables routine detection of far-red IRSL from loess samples.

Acknowledgments

We thank Didier Miallier for his review and valuable comments. ZPL thanks the Clarendon Fund, Oxford University, for full support of his D.Phil. study.

References

Arnold, L., Stokes, S., Bailey, R., Fattahi, M., Colls, A.E., Tucker, G., 2002. Optical dating of potassium feldspar using far-red (λ>665nm) IRSL emissions: A comparative study using fluvial sediments from the Loire River, France. *Quaternary Sciences Reviews*, in press.

Bøtter-Jensen, L., 1997. Luminescence technique: Instrumentation and methods. *Radiation Measurements*, **27**: 749-768.

Colls, A.E.L., 1999. Optical dating of fluvial sediment from the Loire Valley, France. M.Sc. Thesis, University of Oxford, Oxford.

Duller, G.A.T., 1997. Behavioural studies of stimulated luminescence from feldspar. *Radiation Measurements*, **27**: 663-694.

Fattahi, M., 2001. Studies on red thermoluminescence and infra-red stimulated red luminescence. Unpublished D.Phil. thesis, Oxford University.

Fattahi, M., Stokes, S., 2002a. Red luminescence from potassium feldspar stimulated by infrared. *Radiation Measurements*, submitted.

Fattahi, M., Stokes, S., 2002b. Infrared stimulated red luminescence (IRSRL) from potassium feldspar for dating application: a study of some properties relevant for dating. *Radiation Measurements*, in press.

Fattahi, M., Stokes, S., 2002c. Absorbed dose evaluation in feldspar using a single aliquot regenerative-dose (SAR) infrared stimulated red luminescence (IRSL) in potassium feldspar. *Radiation Measurements*, in press.

Huntley, D.J., Lamothe, M., 2001. Ubiquitous of anomalous fading in K-feldspar and the measurement and correction for it on optical dating. *Canadian Journal of Earth Science*, **38**: 1093-1106.

Krbetschek, M.R., Gotze, J., Dietrich, A. Traumann, T., 1997. Spectral information from minerals relevant for luminescence dating. *Radiation Measurements* **27**, 695-748.

Lai, Z.-P., Stokes, S., Bailey, R., Fattahi, M. Arnold, L., 2002. Infrared Stimulated Red Luminescence from Chinese Loess: Basic Observations. *Quaternary Sciences Reviews*, submitted.

Lamothe, M., Auclair, M., 1999. A solution to anomalous fading and age shortfalls in optical dating of feldspar minerals. *Earth and Planetary Science letters*, **171**(3): 319-323.

Miallier, D., Fain, J., Montret, M., Pilleyre, T., Sanzelle, Z., Soumana, S., 1991. Properties of the red TL peak of Quartz relevant to thermoluminescence dating. *Nuclear Tracks and Radiation Measurements*, **18**: 89-94.

Stokes, S., Fattahi, M., 2002. Red emission luminescence from quartz and feldspar: An overview. *Radiation Measurements*, submitted.

Zink, A., Visocekas, R., 1997. Datability of sanidine feldspars using the near-infrared TL emission. *Radiation Measurements* **27**(2), 251-261.

Reviewer

Didier Miallier

Addendum to "Absorbed dose fraction for ^{87}Rb β particles"

M.L. Readhead
Defence Science and Technology Organisation, P.O. Box 44, Pyrmont, NSW, 2009, Australia

(Received 30 September 2002)

This recent paper (Readhead, 2002) calculated the absorbed dose fraction for β particles emitted by ^{87}Rb sources uniformly distributed in a spherical grain of quartz, when surrounded by a region not containing any ^{87}Rb sources. The converse situation, of ^{87}Rb-free quartz grains embedded in an medium uniformly emitting ^{87}Rb β particles, was considered by Adamiec and Aitken (1998). Thinking that an "approximate evaluation of this factor is not available", they "arbitrarily" took the attenuation factor for coarse-grain dating to be 0.75 (see the footnote to Table 8).

The two absorber-emitter situations are complimentary, and a more accurate attenuation factor for the latter case can be obtained from Readhead (2002) by simply replacing Equation 1 with $D_e = N_0 E_0 (1 - S_e)$. Table 1 can then be used to obtain the attenuation factor. For example, for 100 μm diameter grains the attenuation factor is $0.512\,(=1-0.488)$, leading to an absorbed dose of 0.0825×0.512 MeV/N_0 or 0.3580×0.512 μGy/a/(ppm Rb). Note that the attenuation factor differs substantially from the value used by Adamiec and Aitken (1998), although in most dating situations this difference will only have a minor affect on the age of the sample.

Acknowledgement

The author thanks Martin Aitken for bringing his attention to the approximation used in his 1998 paper, and for suggesting this addendum.

References

Adamiec, G. and Aitken, M. (1998). Dose-rate conversion factors: update. *Ancient TL* **16**, 37-50.

Readhead, M.L. (2002). Absorbed dose fraction for ^{87}Rb β particles. *Ancient TL* **20**, 25-28.

A note on the variance of a background-corrected OSL count

Rex Galbraith
Department of Statistical Science, University College London, Gower Street, London WC1E 6BT, U.K.

(Received 14 May 2002; in final form 25 October 2002)

It is common practice to calculate the relative standard error of a background-corrected optically stimulated luminescence (OSL) count by assuming Poisson errors. This note corrects a formula given by Banerjee *et al.* (2000) and suggests alternative formulae for use when the variation in background counts is larger than that implied by the Poisson distribution. For moderately bright samples, the contribution to the relative standard error from estimating the background rate is small, whichever formula is used.

The usual scenario is as follows. Optical stimulation of an aliquot of quartz produces a series of counts - a number of recorded photons for each of N equal length consecutive time intervals (channels). For example, Banerjee *et al.* (2000) used a stimulation period of 60 s with counts in N = 250 channels each lasting 0.24 s. The OSL "signal" is measured from the total count in the first n channels minus an estimate of the contribution to this count from background sources. Often n is taken to be quite small, for example n = 5, corresponding to the first 1.2 s of stimulation. The background emission rate is assumed to be constant over the whole 60 s, and is estimated from counts near the end of this period, where the contribution from the signal is assumed to be negligible.

Mathematically, the above may be expressed as follows. Let y_i denote the OSL count from channel i, for i = 1, 2, …, N, and let $Y_0 = \sum_{i=1}^{n} y_i$ be the total count over the first n channels. Write

$$Y_0 = S_0 + B_0$$

where S_0 and B_0 are the contributions to Y_0 from the signal (or source of interest) and background respectively. Of course S_0 and B_0 are not observed directly. Assume that S_0 and B_0 are independent random quantities with expectations μ_S and μ_B, and variances σ^2_S and σ^2_B, respectively. Then the observed count Y_0 will have expectation $\mu_S + \mu_B$ and variance $\sigma^2_S + \sigma^2_B$. An estimate of the signal μ_S is thus obtained by subtracting an estimate of μ_B from Y_0, i.e.,

$$\hat{\mu}_S = Y_0 - \hat{\mu}_B$$

We want to calculate the relative standard error of this estimate.

An estimate of μ_B is usually obtained from the average OSL count over the last m channels, for some suitable m chosen so that the contribution from the signal is negligible. It is useful to choose m be a multiple of n: let m = nk, say. For example, Banerjee *et al.* (2000) used the last m = 25 channels (6 s) of the series, corresponding to k=5 when n=5. Then let Y_1, Y_2, …, Y_k denote the total counts in the last k sets of n channels, i.e.,

$$Y_j = \sum_{i=N-jn+1}^{N-jn+n} y_i$$

for j = 1, 2, …, k. Thus Y_1, Y_2, …, Y_k are all counts over n channels (the same as for Y_0) and we assume that they are independent random quantities from the same distribution as that of B_0 (i.e., the signal is negligible). In particular, each has expectation μ_B and variance σ^2_B. The estimate of μ_B may then be written as

$$\hat{\mu}_B = \overline{Y} = \frac{1}{k}\sum_{j=1}^{k} Y_j$$

and this has variance $\mathrm{var}(\hat{\mu}_B) = \sigma^2_B / k$ Hence the variance of the estimated signal (corrected for background) is

$$\mathrm{var}(\hat{\mu}_S) = \mathrm{var}(Y_0) + \mathrm{var}(\hat{\mu}_B) = \sigma^2_S + \sigma^2_B + \sigma^2_B / k \qquad (1)$$

and the relative standard error is

$$rse(\hat{\mu}_s) = \frac{\sqrt{\sigma_S^2 + \sigma_B^2 + \sigma_B^2 / k}}{\mu_S} \qquad (2)$$

In order to calculate this relative standard error in practice, we need estimates of σ_S^2 and σ_B^2 in addition to the estimate of μ_S.

In the usual case where Y_0, Y_1 …, Y_k are assumed to have Poisson distributions, $\sigma_S^2 = \mu_S$ and $\sigma_B^2 = \mu_B$. Then (1) becomes

$$\text{var}(\hat{\mu}_S) = \mu_S + \mu_B + \mu_B / k$$

which may be estimated as $Y_0 - \bar{Y} + \bar{Y} + \bar{Y}/k = Y_0 + \bar{Y}/k$. Substituting these estimates into (2) gives the following estimated relative standard error:

$$rse(\hat{\mu}_s) = \frac{\sqrt{Y_0 + \bar{Y} / k}}{Y_0 - \bar{Y}} \qquad (3)$$

This differs slightly from the formula on page 833 of Banerjee *et al.* (2000), where the second term in the numerator is equivalent to $2\bar{Y}/k$. The above argument shows that the factor 2 should not be there.

A drawback with equation (3) in practice is that there is sometimes evidence that the background counts do not have a Poisson distribution, but are over-dispersed (e.g., Galbraith *et al.*, 1999, p 348). For example, the variance

$$s_Y^2 = [\,1/(k-1)] \sum_{j=1}^{k} (Y_j - \bar{Y})^2$$

may be substantially larger than the mean count $\bar{Y}$ (see below). Then we may write

$$\sigma_B^2 = \mu_B + \sigma^2$$

for some positive value of σ^2 to be estimated. An obvious estimate is

$$\hat{\sigma}^2 = s_Y^2 - \bar{Y} \qquad (4)$$

provided this is positive. But there is a drawback with this too: in order to be confident that the contribution to $\bar{Y}$ from the signal is negligible, it might be necessary to use a quite small value of k (e.g., k=5 as above), so that s_Y^2 will be based on a small number of degrees of freedom. A more reliable estimate may be obtained by pooling the background variances for several series. For example, for four series of stimulation with background means $\bar{Y}_1$, $\bar{Y}_2$, $\bar{Y}_3$, $\bar{Y}_4$ and variances s_{Y1}^2, s_{Y2}^2, s_{Y3}^2, s_{Y4}^2, each with k–1 degrees of freedom, one may use

$$\hat{\sigma}^2 = \frac{1}{4}(s_{Y1}^2 + s_{Y2}^2 + s_{Y3}^2 + s_{Y4}^2) - \frac{1}{4}(\bar{Y}_1 + \bar{Y}_2 + \bar{Y}_3 + \bar{Y}_4) \qquad (5)$$

i.e., the average variance minus the average background count for the four series. This pooled estimate of over-dispersion could be used for each series, while at the same time using separate estimates of background level.

It is not so straightforward to obtain a corresponding estimate of σ_S^2 because the expected counts change rapidly at the start of the stimulation period. But there is perhaps a case for assuming that S_0 does have a Poisson distribution, while B_0 does not. The former comes from pure OSL emissions while the latter comes from other sources such as scattered light and instrument noise, which may not exhibit Poisson variation. Then we still have $\sigma_S^2 = \mu_S$ and the resulting estimated relative standard error is

$$rse(\hat{\mu}_S) \approx \frac{\sqrt{Y_0 + \bar{Y} / k + \hat{\sigma}^2(1+1/k)}}{Y_0 - \bar{Y}} \qquad (6)$$

This formula will agree closely with (3) when $\hat{\sigma}^2$ is small, but may be preferable when $\hat{\sigma}^2$ is large.

To get a feel for the numerical consequences, suppose $Y_0 = 12500$ and $\bar{Y} = 50$, with n=5 and k=5. These numbers are comparable with the "bright" sample in Banerjee *et al.* (2000). Suppose also that $\hat{\sigma}^2 = 75$, corresponding to a reasonably substantial amount of over-dispersion ($\sigma_B^2/\mu_B \approx 2.5$). Then the relative standard errors from (3) and (6) are 0.00898 and 0.00902, respectively, which are practically equal. The corresponding absolute standard errors are 111.8 and 112.2. Indeed, if we treated the background as being known *exactly*, the relative standard error of $\hat{\sigma}^2$ would be 0.00896, also practically the same. But for a weak signal, with $Y_0 = 200$ and the same $\bar{Y}$ and $\hat{\sigma}^2$ as above, the two relative standard errors are 0.0966 and 0.1155, and the two absolute standard errors are 14.5 and 17.2. In general, when the signal is weak, equation (6) may give a somewhat larger relative standard error than (3). But when the signal is

strong, both equations give similar answers and in fact the error in estimating the background is practically negligible.

An alternative assumption when there is over-dispersion is that neither S_0 nor B_0 have Poisson distributions, but that the ratio of the variance to the mean is the same for each, i.e., $\sigma_S^2/\mu_S = \sigma_B^2/\mu_B$. It is perhaps hard to think of a physical justification for this: it would imply a multiplicative error mechanism that affected all counts from whatever source. So it would presumably be error associated with the measurement process rather than the process producing the counts. In any case, this would lead to the following estimated relative standard error:

$$rse(\hat{\mu}_S) \approx \sqrt{1+\frac{\hat{\sigma}^2}{\overline{Y}}} \times \frac{\sqrt{Y_0 + \overline{Y}/k}}{Y_0 - \overline{Y}} \qquad (7)$$

where $\hat{\sigma}^2$ is given by (4) or (5). Here equation (3) is multiplied by a factor corresponding to $\sqrt{\sigma_B^2/\mu_B}$. In the above examples this factor would $\sqrt{2.5} \approx 1.6$. In general, this formula is more conservative than (3) or (6).

Some further remarks may be useful. Firstly, there is a simple statistical test for assessing whether the counts Y_1, Y_2, …, Y_k vary consistently with a Poisson distribution. One calculates the Poisson index of dispersion

$$I = (k-1)s_Y^2 / \overline{Y}$$

and assesses its significance from the χ^2 distribution with k−1 degrees of freedom (see for example Kotz and Johnson, 1987, p 25). The quantity I is akin to a χ^2 statistic, a significantly large value of I being evidence of over-dispersion, i.e., the ratio s_Y^2 / $\overline{Y}$ is too large to be consistent with $\sigma_B^2/\mu_B = 1$. Of course there are various ways to test whether data agree with a Poisson distribution; this is a useful method when there is only a small number of counts.

Secondly, estimating a palaeodose typically uses products and ratios of background-corrected OSL counts. Then the approximate relative standard error of the product or ratio is simply obtained by combining the individual relative standard errors in quadrature. For example, for the simplest form of the single-aliquot regenerative-dose protocol,

$$\text{palaeodose} = \frac{s_n}{s_r} \times \frac{t_r}{t_n} \times \text{regenerative dose},$$

where s_n, t_n, s_r and t_r are estimated from background-corrected counts arising from optical stimulation of the natural dose, a subsequent test dose, a regenerative dose and its corresponding test dose, respectively. Then the relative standard error of the palaeodose estimate (assuming the regenerative dose is known exactly) is just the square root of the sum of the squared relative standard errors of the estimates of s_n, t_n, s_r and t_r.

Thirdly, subtracting an estimated background level from a weak signal can produce inappropriate estimates. An alternative approach is to estimate the signal *in the presence of* the background using statistical models (e.g., Galbraith *et al.*, 1999).

Finally, when estimating palaeodoses or other OSL parameters from several aliquots of quartz, whether using single- or multiple-aliquot methods, there are usually other sources of variation to account for in addition to those reflected in (3), (6) or (7). These may be more substantial and work on estimating them is in progress.

I thank John Prescott, Bert Roberts and Andrew Murray for useful comments on an earlier version of this note.

References

Banerjee, D., Bøtter-Jensen, L. & Murray, A.S. (2000) Retrospective dosimetry: estimation of the dose to quartz using the single-aliquot regenerative-dose protocol. *Applied Radiation and Isotopes*, **52,** 831-844.

Galbraith, R.F., Roberts, R.G., Laslett, G.M., Yoshida, H. and Olley, J.M. (1999) Optical dating of single and multiple grains of quartz from Jinmium rock shelter, Northern Australia: Part I, Experimental design and statistical models. *Archaeometry*, **41,** 338-364.

Kotz,S. & Johnson, N.L., Editors (1987) Poisson Index of Dispersion. *Encyclopedia of Statistical Sciences*, volume 7, Wiley 1987.

Reviewer

John Prescott

The luminescence dating laboratory at the University of Bonn: equipment and procedures

B. Mauz*, T. Bode, E. Mainz, H. Blanchard, W. Hilger, R. Dikau and L. Zöller
Geographisches Institut University of Bonn, Meckenheimer Allee 166, D- 53115 Bonn, Germany, *corresponding author: email bmauz@giub.uni-bonn.de

(Received 4 March 2002 ; in final form 25 November 2002)

Abstract: *This paper documents the facilities and procedures used for luminescence dating in the laboratory of the Department of Geography at the University of Bonn. We focus on optically stimulated luminescence (OSL) dating of fine-sand quartz samples and infrared stimulated luminescence (IR-OSL) dating of polymineral fine-silt samples.*

Introduction

The luminescence dating laboratory at the University of Bonn is situated in the Department of Geography where it is part of the working group focusing on geomorphology and Quaternary geology. The major task of the laboratory is to provide age data for internal research projects and to contribute to luminescence dating research. Moreover, it is expected to conduct dating for external research projects. The laboratory is able to carry out dating of aeolian deposits, fluvial and colluvial deposits and coastal deposits using fine-sand quartz and feldspar grains (100-250 µm, commonly called "coarse grained") or polymineral fine-silt (4-11 µm, commonly called "fine grained") extracted from the sample.

A number of laboratories with similar capacities and objectives exist. Essential procedures used in these laboratories are mostly reported together with the scientific results. It is the purpose of this paper to present the facilities, equipment, essential parameters, sample procedures, tests for D_e reliability and assessments of uncertainties used in our laboratory and in doing so, to push forward standardisation in luminescence dating.

Facilities and equipment

Laboratory light

Quartz samples are treated under subdued yellow or red light. Yellow light is provided by a low pressure Na-lamp (Osram MW 18W, monochromatic sodium doublet at 589 nm, Spooner et al., 2000) filtered with a Schott OG530/3mm filter to cut the weak blue emission of the lamp. Red light is provided by red light emitting diodes (LED type Siemens LS5421-Q) filtered with a Hoya R62/3mm filter (Figure 1, Schilles, 1998). Feldspar and fine-silt samples are treated under subdued yellow or green light; the latter is provided by one LED (type Nichia NSPG-500) filtered with a Schott OG 515 filter (Figure 1, Schilles, 1998). Routinely, light does not directly fall onto the sample being prepared. All light sources were tested using two fine-silt loess samples from Germany and Pakistan (laboratory codes: BN181 and BN80, respectively, prepared as indicated in section 3), and a fine-sand quartz sample from the Sahara (laboratory code BN202, prepared as indicated in section 3). The quartz sample was subsequently manually powdered to grains < 15 µm and was settled onto aluminium discs. In Figure 2 the results of the tests of the LED-lamps and the Na-lamp are shown: none of the light sources are able to bleach the sample within 20h.

Beta-sources

The laboratory has two beta sources at its disposal:
1) a stand-alone Amersham $^{90}Sr/^{90}Y$ β-source (3.7 GBq) mounted in a Littlemore device delivering 7.5±0.4 Gy min^{-1} (calibrated on "date", i.e. value related to the calibration datum) to fine-silt sample material on 5 mm thick aluminium discs.
2) a Amersham $^{90}Sr/^{90}Y$ β-source (1.5 GBq) mounted in the luminescence reader delivering 5.9±0.09 Gy min^{-1} (calibrated on "date") to 90-300 µm quartz grains mounted on 5 mm thick stainless steel discs. The strength of the source can be reduced to a minimum dose rate of ~0.76 Gy min^{-1} by fitting aluminium discs of different thickness underneath the source.

Both β-sources were calibrated using loess and quartz material respectively, irradiated by the ^{137}Cs γ-source of the Risø Laboratory (Denmark). This γ-source delivers an accurately known dose rate of about 0.10 Gy h^{-1} in air (A.S. Murray, pers. com.). The calibration dose of the quartz sample is 4.59±0.07 Gy, that of the loess sample is 8.51±0.13 Gy.

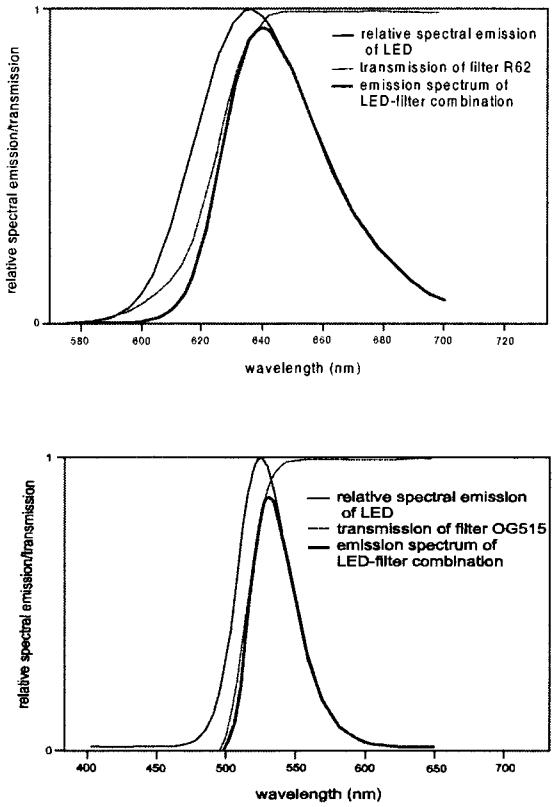

Figure 1.
Spectral curves of LED laboratory light (Schilles, 1998). A: red LEDs; B: green-yellow LEDs

Alpha-sources

Six ^{241}Am sources (3.7 MeV) are mounted in a self-made unit controlled by a self-made electronic box. The sources have been calibrated using TLD 200 and cross-checked with α-sources of the same type in the Forschungsstelle Archaeometrie at Heidelberg. The mean source strength was 0.2018 μm^{-2} min which resulted in 2.62 Gy min^{-1} being delivered to fine-silt (4-11 μm) TLD 200 deposited on aluminium discs as a monolayer (Bürgi, 1992). Irradiation is administered at 10 mm distance to the discs under vacuum (10^{-4} mbar).

Luminescence readers

1) Daybreak 1100 automated TL/IR-OSL System equipped with 10 IR-LEDs (845Δ20 nm), and a 300 W Xe arc lamp. This is used for fine-silt sediments.

2) Risø automated TL/OSL System, DA-15 equipped with a β-source, a 1W IR-laser diode (830Δ20 nm, delivering ~250 mW cm^{-2}) and 42 blue LEDs (470□20 nm, delivering ~50 mW cm^{-2} when running at full power). This is used for sand-sized quartz and feldspars.

Gamma-spectrometer

The low level γ-spectrometer is characterised by the following data:

- DSG coaxial HPGe detector, n-type
- Detector size: 58.2 mm diameter and 57.8 mm high
- Entrance window: Mylar, at ~5mm distance from the Ge-crystal
- Energy resolution: FWHM at 122 keV : 0.87 keV, FWHM at 133 MeV: 1.86 keV
- Efficiency: 33.2%
- Peak to Compton: 58.4:1.0

The detector is shielded with 5 mm perspex, 15 mm copper and 15cm low activity Pb. A perspex bar guarantees exact positioning of the sample and the reference material onto the detector (Figure 3).

Alpha-counter

The laboratory has a Littlemore Low Level Alpha Counter 7286 equipped with 2 photomultiplier tubes (EMI type 6097). This device is based on scintillator techniques where light is produced by an α-particle interacting with a zinc sulphide screen. The light is collected by a photomultiplier tube.

Beta-counter

Kind collaboration allows us to use occasionally the β-counter in the Department of Geography at the University of Cologne. The equipment is a Risø low level GM 25-5 multicounter system equipped with five individual sample counters and a guard counter. The device is based on Geiger-Müller counting and anticoincidence techniques to reduce the cosmic ray background. Reference material is loess material (Table 1) for external beta dose determination and KCl granulat for internal beta dose determination.

Sample preparation

Fine-silt

The fine-silt preparation aims to separate 4 – 11 μm grains from the sample. The following steps are carried out:

1) sieving of the fraction < 63 μm; 2) H_2O_2 treatment to remove organic material starting with H_2O_2 10% in order to control heating of the sample and continuing with H_2O_2 35% after a weak alkaline pH (~8) is produced using NaOH-liquid; 3) settling in 0.01 N NH_3 in Atterberg cylinders to remove grains > 11 μm and grains < 4 μm using Stokes' Law. If the sample is rich in clay, it is shacken for around 12h before the separation process is started. The settling process is repeated as often as necessary to guarantee the completeness of the grain size separation; 4) dissolution of carbonate using CH_3COOH 20%; 5) settling the sample onto aluminium discs using the material suspended in water. During all preparation steps in which acids or alkaline solutions are involved, the pH is continuously monitored.

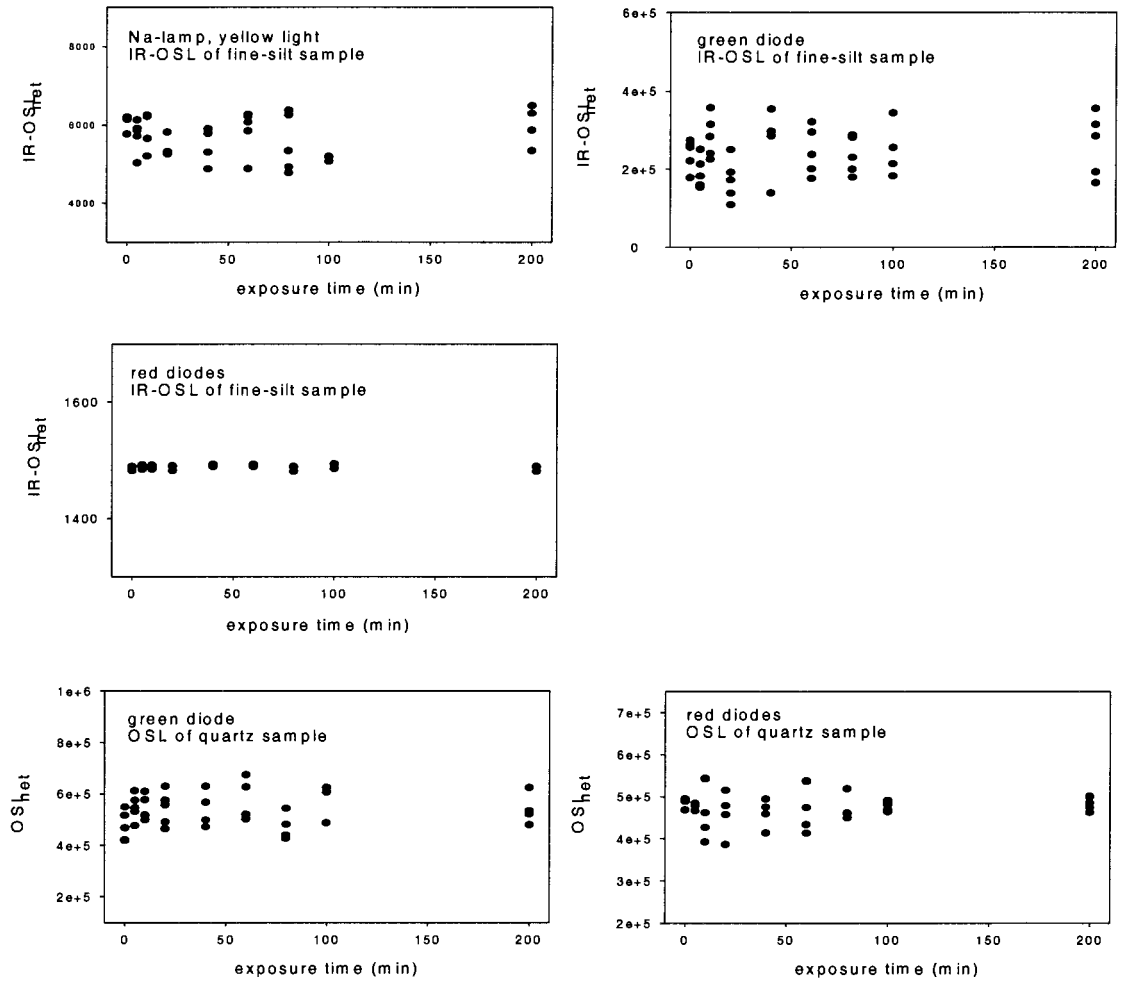

Figure 2.
Test of laboratory light sources. IR-OSL$_{net}$ = signal integral of the first 10 s subtracted from the background; OSL$_{net}$ = signal integral of the first 1.2 s subtracted from the background. Loess samples: normalisation using 0.1 s natural IR-OSL before exposure to light; 60 s IR-OSL of the natural dose; Quartz sample: 46 Gy was added to the natural dose by laboratory irradiation, followed by a preheat of 260°C for 10 s and 0.1 s OSL before exposure to laboratory light. Distance between light source and sample and intensity of light was chosen according to routine working circumstances (~50 cm distance).

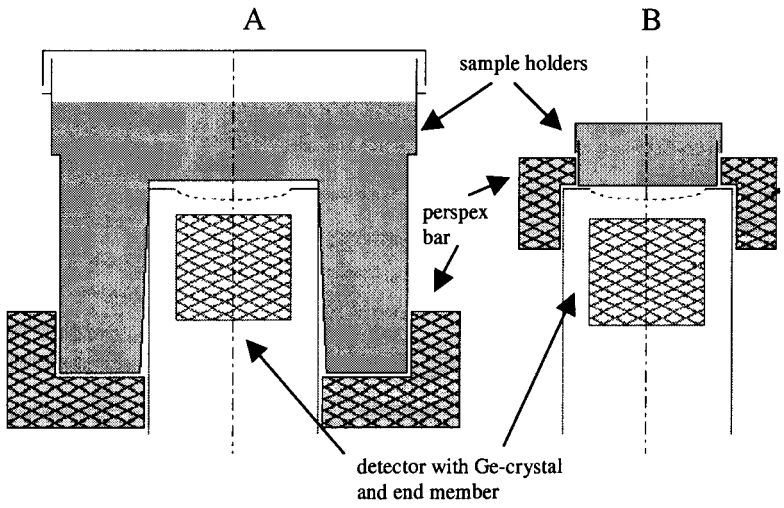

Figure 3.
Design of the γ-spectrometer detection unit. A Marinelli beaker, B plastic sample holder

Fine-sand

This procedure aims to separate a monomineralic quartz or K-rich feldspar subsample in the grain size 100 – 250 µm. The following steps are carried out: 1) sieving out the fine sand fraction according to the grain size composition of the sample. We prefer restricted fractions (e.g. 160-200 µm); 2) H_2O_2 treatment to remove organic material starting with H_2O_2 10% in order to control heating of the sample and continuing with H_2O_2 35% after a weak alkaline pH (~8) is produced using NaOH-liquid; 3) dissolution of carbonate using CH_3COOH 20% or HCl; 4) density separation using sodium polytungstate to eliminate heavy minerals and to separate quartz (2.70 - 2.62 g cm^{-3}) from K-rich feldspars (< 2.58 g cm^{-3}); 5) etching the quartz grains in 40% HF for 80 min while stirring the grains. Etched grains are treated subsequently in 10% HCl and sieved to > 100 µm to remove broken grains; 6) spreading grains onto stainless steel discs; the amount of material is chosen according to the bleaching history of the sediment and the brightness of the mineral.

Detection filters

Generally, IR-OSL of feldspars is detected in the blue wavelength range using Schott 2xBG3/3 mm, BG39/3 mm, GG400/3 mm filters (Krbetschek et al., 1996). The filter combination transmits 390-450 nm and thus encompasses the 410 nm-emission. OSL of quartz is detected in the UV wavelength range using Hoya U340/7.5mm filter glass transmitting between 290 and 380 nm.

D_e determination

Fine-sand K-rich feldspar and polymineral fine-silt samples

Routinely, these samples are measured using a multiple aliquot additive dose protocol. We prepare 80 aliquots of a sample: 40 aliquots are used to determine De_β (10 aliquots for L_N and 6x5 aliquots for increasing $L_N+\beta$, e.g. Figure 4) 3x3 aliquots receive an increasing additive α-dose and 10 to 25 aliquots are reserved for anomalous fading test A and test B (see section 6). All samples are normalised before any treatment using a 0.1 to 0.2 s stimulation time according to the brightness of the dosimeter. All samples are stored at room temperature for at least 30 d after irradiation.

Fine-sand quartz

These samples are measured using a single-aliquot regenerative-dose (SAR) protocol. If possible (e.g. enough material available), a preheat test is

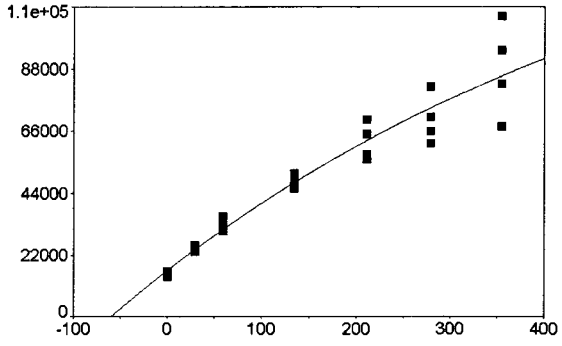

Figure 4.

Dose response curve and D_e determination of the loess sample (BN181) using multiple aliquot additive dose protocol. The sample was stored 40 d after irradiation, the preheat was 280°C for 10 s; IR-OSL_{net} = signal integral of the first 10 s subtracted from the background

conducted between 200°C and 300°C for 10 s to determine the optimal preheat procedure. Routinely, a preheat of 260°C for 10 s is used for L_x and 220°C for 10 s for T_x. The amount of recuperation is calculated from $\frac{L_N}{T_N} / \frac{L_0}{T_0}$, where L_N is the natural OSL and L_0 is the zero OSL of the SAR protocol (Murray and Wintle 2000, e.g. Table 2); The recycling ratio is determined from the ratio of the first regenerated dose and the repeated first regenerated dose at the end of the SAR-run (e.g. Table 2). Sensitivity change during a SAR run is corrected by a test dose OSL (T_x). The reliability of this correction is checked by plotting L_x versus T_x of a SAR protocol in which an equal beta-dose is administered for 6 times (Figure 5C).This run is conducted with aliquots used for D_e-determination without treating them further. The L_x/T_x relationship is expressed as Pearson's correlation coefficient (e.g. Table 2) and should be linear to zero. Figure 5C shows the robustness of SAR even if the test dose does not lay in the optimal dose range. If possible, D_e(t)-plots are produced over the entire stimulation time and the reliability of D_e estimation is checked according to the stimulation time chosen for D_e estimation (e.g. Table 2, Figure 5D). If necessary, a dose recovery is conducted, where a given dose similar to the estimated D_e is recovered. The same aliquots and the same SAR protocol used for D_e determination are used and the aliquots are not treated before administering the laboratory dose (e.g. Table 2).

Tests for contamination and for anomalous fading

Several tests are carried out to control the D_e result:

laboratory	technique	U [µg/g]	Th [µg/g]	K [wt%]	$\dot{D}_\alpha$	$\dot{D}_\beta$	$\dot{D}_\gamma$	D_e
FSA	low level γ-spec	3.32±0.24	8.21±0.85	1.20±0.09	12.25±0.74	1.67±0.08	1.10±0.06	62.4±5.4
MPI	NAA	3.00±0.11	8.09±0.09	1.19±0.03	11.48±0.25	1.61±0.03	1.05±0.02	-
MPI	NAA	2.80±0.08	8.27±0.09	1.19±0.04	11.16±0.18	1.59±0.03	1.04±0.01	-
MPI	NAA	2.84±0.17	8.09±0.24	1.18±0.05	11.13±0.40	1.58±0.05	1.03±0.03	-
SAW	low level γ-spec	3.00±0.10	7.42±0.32	1.07±0.06	11.07±0.29	1.50±0.05	0.99±0.02	-
	low level γ-spec	2.99±0.40	7.50±1.20	1.64±0.28	11.10±0.14	1.95±0.23	1.13±0.10	-
Bonn	low level γ-spec	3.12±0.05	8.50±0.10	1.09±0.04	12.0±0.13	1.56±0.03	1.02±0.01	59.8±14.6

Table 1.

Comparison of analytical data for the loess sample (BN181). Sample material used in this study has been collected subsequent to previous analysis and the sample was collected at a position only a few decimetres from the previous sampling position. Data from the other laboratories are unpublished.

FSA = Forschungsstelle Archaeometrie der Heidelberger Akademie der Wissenschaften, data provided by A. Lang (1997).

MPI = Max-Planck-Institut für Kernphysik in Heidelberg, data provided by E. Pernicka (1995).

SAW = Saechsische Akademie der Wissenschaften, data provided by J. Heinecke (1996).

Table 2.

Analytical data of BN169. Moisture factor is the measured field moisture normalised to the dry mass and corrected for fluctuation of water content; n indicates the number of measured aliquots; Recuperation is given in % of $\frac{L_0}{T_0} / \frac{L_N}{T_N}$*; recycling ratio is the ratio of the repeated first regenerated dose at the end of the SAR protocol and first regenerated dose; Sensitivity change is a check of the correction procedure during SAR by the relationship of* L_x *and* T_x *after equal beta-dose for 6 times. The term is expressed in correlation coefficient. Dose recovery is given as recovered dose/laboratory dose.* $D_e(t)$ *indicates the stimulation time range (s), where* D_e *is onstant (1*σ*). IR-sensitivity indicates a feldspar component of the quartz dosimeter by the ratio* $\frac{Lp}{Tp} / \frac{L}{T}$*. Age is indicated with 1* σ *total uncertainty.*

For further explanations see text.

Moisture factor	1.15±0.10
grain size (µm)	160-200
U (µg g^{-1})	0.28±0.026
Th (µg g^{-1})	0.69±0.07
K (wt %)	0.44±0.01
$\dot{D}_{cosm}$ (Gy ka^{-1})	0.18±0.009
$\dot{D}_{effective}$ (Gy ka^{-1})	0.65±0.04
D_e (Gy)	6.05±0.17
n	21
recuperation (%)	0.11±0.02
recycling ratio	1.000±0.002
sensitivity change correction	0.70±0.04
dose recovery	1.03±0.03
$D_e(t)$ (s)	0 - 2
IR sensitivity	1.02±0.10
age (±1σ, ka)	9.30±0.68

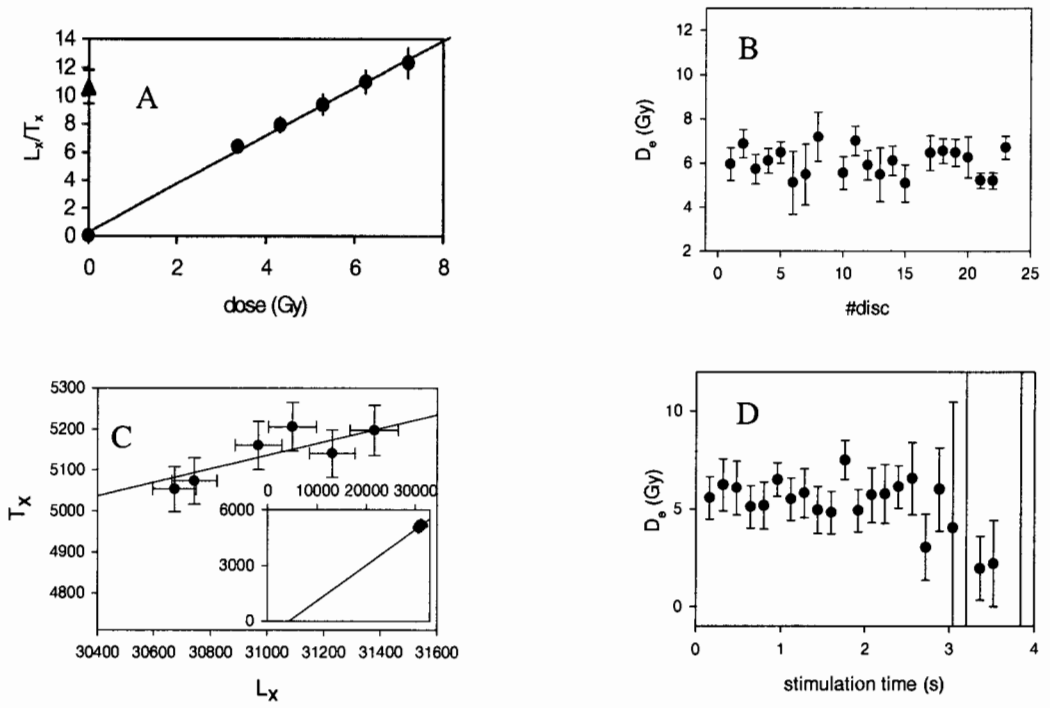

Figure 5.

D_e determination and D_e reliability tests of the quartz sample BN169 using SAR protocol. A: dose response curve with circle=regenerated dose response using a single exponential saturation function, triangle= natural OSL. Data points are calculated as mean and standard deviation of 21 aliquots; B: dose distribution of 21 aliquots; C: plot of L_x versus T_x as a control of the sensitivity change correction procedure in SAR. Test dose was around 10% of the expected D_e (~0.48 Gy). Inset shows the same data set extrapolated to the x-axis; D: $D_e(t)$ plot of aliquot 22.

energy (keV)	nuclide	group and parent
583.2	^{208}Tl	group I: ^{232}Th
2614.5	^{208}Tl	
238.6	^{212}Pb	
911.2	^{228}Ac	group II: ^{232}Th
338.3	^{228}Ac	
969.0	^{228}Ac	
609.3	^{214}Bi	group I: ^{238}U
1120.0	^{214}Bi	
1764.5	^{214}Bi	
295.2	^{214}Pb	
351.9	^{214}Pb	group II: ^{238}U
63.3	^{234}Th	
46.5	^{210}Pb	
1460.8	^{40}K	^{40}K

Table 3.

Energy lines and daughter nuclides in secular equilibrium used to determine weighted mean of equivalent total U- and Th activity and ^{40}K activity. Data set and calibration of the spectrometer is based on the Nuclear Science Reference file.

Feldspar contamination of quartz:
Before conducting a SAR sequence for D_e-determination around 15 aliquots used for other tests are given a laboratory dose equivalent to the expected D_e and the OSL normalised to a test dose is measured ($\frac{L}{T}$). Subsequently the same aliquots are given the same laboratory dose as before and the post-IR OSL normalised to a test dose is measured ($\frac{Lp}{Tp}$). The ratio $\frac{L}{T}/\frac{Lp}{Tp} > 1$ indicates a feldspar component in the OSL signal (Henshilwood et al., 2002).

Anomalous fading
Tests for anomalous fading are performed on all feldspar samples. Two test protocols are used in our laboratory: Test A is routinely applied to all samples. Test B is performed, if test A shows a ratio of < 0.9.
Test A: This test is incorporated in the multiple aliquot additive dose protocol. A set of 5 aliquots with the natural dose (L_N) and 5 aliquots containing the maximum additive dose ($L_N+\beta_{max}$) used for D_e-determination are preheated at 280°C for 10 s and subsequently stored at room temperature for around three months (t~2200h). The amount of anomalous fading is then given by the ratio:

$$\left(\frac{L_N + \beta_{max}}{L_N}\right)_{stored} / \left(\frac{L_N + \beta_{max}}{L_N}\right)_{unstored} \quad (1)$$

which is the ratio between the aliquots stored for ~2200 h and the aliquots stored for ~720 h.
Test B: A set of 20 aliquots are used: 10 aliquots for L_N and 10 aliquots for $L_N+\beta_{max}$, and further 5 aliquots are used to correct for optical erosion of L_N and $L_N+\beta_{max}$. We use t_1=2d, t_2=storage time of aliquots used for D_e-determination (~30d), t_3=40d, t_4=50d, t_6=60d and plot $\frac{L_N + \beta_{max}}{L_N}$ versus storage time. The slope of the regression line indicates the amount of signal loss over LN(t). Yet, we do not correct ages by fading rates determined (Huntley and Lamothe, 2001) but need more experiences to do so. The age of a sample showing a significant fading rate is indicated with its minimum age (a_{min}) given as a_{min}= a-2σ where 2σ is the 95% confidence interval.

Dose rate determination
The dose rate is produced by the activity of natural radionuclides in the sample and its immediate environment. Our laboratory determines the specific activity (Bq kg^{-1}) of a sample using low level γ-spectrometry. The specific activity ($A_s(t)$) is subsequently transformed into concentration (A^*_s, µg g^{-1} and wt%) following

$$A^*_s(t) = \frac{1000\ m_a}{\lambda N_A} A_s\ (t) \quad (2)$$

where N_A = Avogadro constant, m_a=atomic weight (n) and $\lambda = \tau^{-1}$ (decay constant) multiplied by the conversion factors of Adamiec and Aitken (1998) to obtain the dose rate for each isotopic chain. The calculated $\dot{D}_\alpha$ and $\dot{D}_\beta$ are occasionally checked by thick source α-counting and β-counting respectively. The accuracy of a dose rate value determined in this way, is largely dependent on the γ-spectrometer technique, the reference material and the activity of the sample. Our laboratory uses:

low level γ-spectrometry:
Samples are packed into air-tight plastic boxes holding around 100 g and stored for ~3 weeks in order to achieve secular equilibrium between ^{226}Ra and ^{222}Rn. Routine measurement time is ~70h. Energy lines of the γ-spectrum are selected according to (1) detector efficiency, (2) specific line intensities, (3) expected nuclide concentrations, (4) superposition of energy lines, (5) position of the Compton edge, (6) self-absorption of the sample. Selected energy lines are shown in Table 3. An experiment designed as a qualitative check showed that, in the low energy range, self-absorption may become significant. The increasing background in this energy range together with increasing self-absorption reduces the precision of energy lines <100 keV. We believe therefore, that secular disequilibrium can only be assessed qualitatively.
The reference material used is: BfS ST2.3/Boden/V-98. This is a soil material provided by the 'Physikalisch-Technische Bundesanstalt' (Schkade et al., 1998).

a-value
The a-value is determined using: $\frac{D_{e\beta}}{D_{e\alpha}}$ according to the a-value system of Aitken (1985), where

$$a_{3.7} = \frac{L}{Gy\alpha}/\frac{L}{Gy\beta} \quad (3)$$

$a_{3.7}$ = a-value resulting from the ^{241}Am α-source delivering 3.7 MeV, $\frac{L}{Gy(\alpha,\beta)}$ = luminescence per Gy α– or β– irradiation. $D_{e\alpha}$ is determined using six ^{241}Am sources and administering 3 different additive

doses on a separate set of aliquots containing fine–silt material. The α-doses chosen encompass the $D_{e\beta}$ of the sample. Cosmic ray contribution ($\dot{D}_{cos}$) is estimated using of the average burial depth of the sample (Prescott and Hutton, 1994). The internal dose rate of K-rich feldspars ($\dot{D}_i$) is determined using β-counting of the grains used for D_e estimation.

Total dose rate

The total dose rate of a quartz sample is calculated as the sum of $\dot{D}_\beta$, $\dot{D}_\gamma$ and $\dot{D}_{cos}$ assuming a negligible contribution of $\dot{D}_\alpha$ due to the HF-treatment of the grains. The total dose rate of a K-rich feldspar sample is the sum of $\dot{D}_\alpha$, $\dot{D}_\beta$, $\dot{D}_\gamma$, $\dot{D}_i$ and $\dot{D}_{cos}$ allowing for a $\dot{D}_\alpha$ contribution from 1/3 of the grain volume and an a-value assumed of 0.08±0.02. For both quartz and feldspar samples $\dot{D}_\beta$ is corrected with the attenuation factors for U, Th and K following Mejdahl (1979). The total dose rate of a fine-silt sample is the sum of $\dot{D}_\alpha$, $\dot{D}_\beta$, $\dot{D}_\gamma$ and $\dot{D}_{cos}$ The effective dose rate of all sample types described here results from correcting $\dot{D}_\alpha$, $\dot{D}_\beta$ and $\dot{D}_\gamma$ with the moisture factor (Aitken, 1985).

Uncertainties

The total uncertainty of an age determined is given by systematic and random errors. Sources of uncertainties are:

Water content: this value is estimated according to the field moisture monitored immediately after sampling, the pore volume estimated and the assessment of water content fluctuation over the time range to be determined. The latter is expressed by the uncertainty of the moisture factor.

γ-spectrometry: the uncertainty results from the fit (peak areas of the sample, of the reference material and of the background) and the effect of the background on the counting statistics of the sample. We assume similar and comparable sample geometry, chemical composition and mass between reference material and sample. The samples are measured as long as is needed to achieve a sufficiently low (<5%) statistical uncertainty in the peak areas. The value to be used for dose rate determination is calculated as the weighted mean of the energy lines that are in secular equilibrium (Table 3).

Beta source calibration: this uncertainty is calculated using Gaussian error progradation (equation 4) with the error of the reference source (here: Risø ^{137}Cs-source) and the error of the calibration measurement (counting statistics).

Internal activity of quartz: following Aitken (1985) a value of 0.03 Gy ka^{-1} is added to the total dose rate uncertainty.

SAR: in the SAR protocol, uncertainties result from L_x, Bg_{Lx}, T_x, Bg_{Tx}, (Bg=background), calculated using $\sqrt{n}$ and each parameter of the regression analysis. Gaussian error propagation is used to determine the uncertainty of each aliquot. The uncertainty of D_e is then given as standard deviation of n measurements where n ≥ 24 including beta source calibration uncertainty.

Multiple aliquot: in the multiple aliquot additive dose protocol, the error of D_e is given by the disc-to-disc scatter, each parameter of the regression analysis and beta source calibration uncertainty.
Uncertainties are calculated using

$$\Delta F(x_1....x_n) = \pm \sqrt{\sum_{i=1}^{n} \left(\frac{\delta F(x1...xn)}{\delta xi} \Delta xi\right)^2} \qquad (4):$$

where F = function, x = variable and Δx = absolute error of x.

Test of reliability of D_e determination in Bonn

Here, we show two examples of data sets used to control the laboratory procedures.

D_e of a polymineral fine-silt sample

The sample BN181 is a loess sample from the locality Nussloch (S-Germany). The sample was collected from calcareous loess overlying the Eltville Tephra. The age of the sample was expected to be younger than the Tephra, which has been dated to 22±3 ka (Zöller *et al.*, 1988, Hatté *et al.*, 1999), and older than ~15 ka, when loess deposition ended in this area. This sample has been analysed by a number of luminescence dating laboratories in Germany. From this comparison (unpublished) the D_e was expected to be ~60 Gy and IR-OSL age to be ~19 ka. Using multiple aliquot additive dose protocol and a preheat of 280°C for 10 s our laboratory determined 59.8±14.6 Gy (Table 1, Figure 4).

D_e of a fine-sand quartz sample

The quartz sample BN169 originates from a sandy dune layer in N-Germany, which was subject to podzolic alteration. This kind of soil forming process (dominantly vertical transport of Al and Fe in an acid

environment) should not alter the quartz grains, so that OSL is expected to date the time of dune sand deposition. The AMS ^{14}C age of a charcoal incorporated in this podzolic dune layer is 9.53±0.05 cal ka BP (Müller, 2000). According to the temporal relationship between sand deposition, soil formation and incorporation of the charcoal piece in the soil, the OSL age must be slightly lower than the ^{14}C age. Our laboratory determined 9.3±0.7 ka. All analytical data of the sample are given in Table 2.

Conclusion

It is shown, that the essential parameters in the luminescence laboratory of Bonn are accurate but that precision has to be improved.

We note here, that certificate reference material for α-counting, β-counting and γ-spectrometry is not available. Moreover, uncertainty calculations and fading tests and herein the time interval of observation need to be standardised. We feel, that reference material should be produced and more standards should be introduced in order to improve comparison in luminescence dating.

Acknowledgements

We thank B. Pernicka, J. Heinicke and A. Lang for providing data for comparison purposes. We further thank H. Böttger and R. Müller-Geiger for supporting the laboratory by their technical and administrative input. We are grateful to Ann Wintle for discussing an early draft of the manuscript, correcting the English and for giving helpful comments. The equipment has been purchased with the help of the University of Bonn, the Deutsche Forschungsgemeinschaft and the Ministry of Education and Science of Nordrhein-Westfalen.

References

Aitken, M. J. (1985). Thermoluminescence dating. Academic Press, London, 359 pp.

Adamiec, G. and Aitken, M. (1998). Dose-rate conversion factors: update. *Ancient TL*, **16-**(2), 37-50.

Bürgi, K.A. (1992). Aufbau und Betrieb eines Theromlumineszenz-Labors zur Datierung quartärgeologischer Proben. Ph thesis, University of Bern, unpublished.

Hatté, C., Antoine, P., Fontugne, M., Rousseau, D., Tisnérat-Laborde, N., Zöller,L., (1999). New chronology and organic matter δ C-13 paleoclimatic significance of Nußloch loess sequence (Rhine Valley, Germany). *Quaternary International* **62**, 85-91.

Henshilwood, C.S., d'Errico, F., Yates, R., Jacobs, Z., Tribolo, C., Duller, G.A.T., Mercier, N., Sealy, J.C., Valladas, H., Watts, I. and Wintle, A.G. (2002). Emergence of modern human behaviour: Middle stone age engravings from South Africa. *Science* **295**, 1278-1280.

Huntley, D. and Lamothe, M. (2001). Ubiquity of anomalous fading in K-feldspars, and the measurement and correction for it in optical dating. *Canadian Journal of Earth Sciences* **38**, 1093-1106.

Krbetschek, M. R., Rieser, U. and Stolz, W. (1996): Optical Dating: Some Luminescence properties of natural feldspars. *Radiation Protection Dosimetry* **66**, 407-412.

Mejdahl, V. (1979). Thermoluminescence dating: Beta-dose attenuation in quartz grains. *Archaeometry* **21**, 61-73.

Müller, M.J. (2000). Altersbestimmung an schleswig-holsteinischen Binnendünen mit Hilfe von Paläoböden. *Trierer Bodenkundliche Schriften*, **1**, 23-31.

Murray, A.S. and Wintle, A.G. (2000). Luminescence dating of quartz using an improved single-aliquot regenerative-dose protocol. Radiation Measurements 32, 57-73.

Prescott, J. R. and J. T. Hutton (1994). Cosmic ray contribution to dose rates for luminescence and ESR dating: Large depths and long-term time variations. *Radiation Measurements*, **23**, 497-500.

Schilles, T. (1998). Entwicklung und Anwendung einer Technik zur 'Single Aliquot' Datierung mittels Optisch Stimulierter Lumineszenz. Diploma thesis, University of Heidelberg, unpublished.

Schkade, U.-K., Arnold, D., Hartmann, M. and Naumann, M. (1998). Gammaspektrometrische Bestimmung der spezifischen Aktivität natürlicher Radionuklide in Umweltproben. PTB Internal Publication.

Spooner, N.A., Questiaux, D.G. and Aitken, M.J. (2000). The use of sodium lamps for low-intensity laboratory safelighting for optical dating. *Ancient TL* **18**, 45-49.

Zöller, L., Stremme, H.E. und Wagner, G.A. (1988). Thermolumineszenz-Datierung an Löß-Paläoboden-Sequenzen von Nieder-, Mittel- und Oberrhein. *Chemical Geology (Isot. Geosc. Sect.)* **73**, 39-62.

Reviewer

M. Lamothe

Technical note:

A stable reference light source

J. Faïn, D. Miallier, S. Sanzelle, T. Pilleyre
Laboratoire de Physique Corpusculaire, 63177 Aubière cedex, France

Introduction

In the course of luminescence experiments, it can sometimes be useful to check the long term stability of the system which measures the emitted light. This means that, for a given luminescent sample, the counting must be the same whatever the amount of time that has elapsed between two successive measurements. The problem arise, for example, in fading tests or in day light bleaching studies, which involve repeated measurements of a given sample, day after day or month after month.

For that purpose, we have been using for several years a stable light source that can be simply measured at any time for checking a possible shift in the light detection system, and correcting for such a shift in the case it is significant. It is presented below.

Basically, the light source is a scintillating screen that is irradiated by beta particles from ^{14}C nuclei. The design that is given on Fig.1 is only schematic, since the geometry and size will depend on the luminescence set that is used.

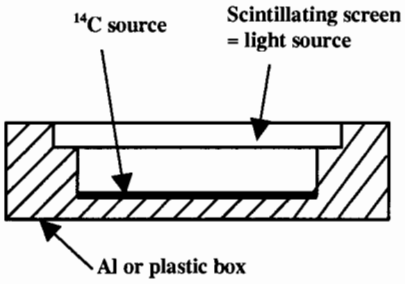

Figure 1.
Schematic cross section of the light source

The ideal reference light must have the same features as the samples to be measured : same order of magnitude of counting rate and same colour, so that all possible causes of shift in the measuring system are taken into account, including, e.g., slight variation of the response of the PM tube (due to electronic shift) or variation of the transparency of the front filter (due to scratching, or darkening during TL experiments).

In this view, two different screens are used in our laboratory for routine TL dating of quartz in the red or in the blue region of its spectrum.

The blue one is a *general purpose* polyvinyl toluene plastic sheet (Nuclear Enterprise NE 102), 1 mm thick, with luminescence emission at around 420 nm.

The red one is a europium doped LuAg ($Lu_3Al_5O_{12}:Eu^{3+}$), 1 mm thick, which has a luminescence at around 620 nm. This is the wavelength of the main red emission of quartz (see, e.g., Hashimoto et al., 1987). It should be noted that this material is not commercially available, however it can be processed quite easily by a specialized laboratory since it has the same features as the famous YAG: Nd^{3+} used in lasers. However, authors can help providing a few of them.

Both screens are stable. Particularly, LuAg is chemically and mechanically very resistant and not hygroscopic. It can possibly shift a little with temperature, but not significantly around room temperature. When compared with YAG, substitution of Y by Lu is intended to enhance the absorption of ionising radiation, thus to increase efficiency.

Choice of the beta source

When the current delivered by the photo-multiplier tube is used for luminescence measurements, no special specification has to be followed in the design of the reference light-source. But, when the photo-multiplier tube is routinely used in the photon counting mode, special care must be given to the choice of the beta source, for both activity and beta energy considerations: typically, less than one photo-electron should be emitted by the photo-cathode per beta particle incident to the scintillating screen, at a rate lower than the routine counting frequency. This requires not too high an energy – ^{14}C fits this condition - and a limited activity. The reason why is qualitatively explained below.

Suppose 10 photons reach the photo-cathode for one incident beta particle. Since they all arrive at the same time, this will result in a single pulse initiated by the simultaneous production of 2 photo-electrons (assuming a 20% quantum efficiency). If less than 10

photons reach the cathode, due to variation of the filter transparency, or if the efficiency of the photo-multiplier shifts and becomes lower say by a factor of 2, the bunch of 10 photons still will result in one pulse, initiated by 1 photo-electron only. The pulse will have twice a lower intensity, but the counting rate with a given beta source will remain unchanged, leaving the operator unaware of the shift. However, with a TL or OSL source, which gives randomly time-distributed photons, the counting rate will have been reduced by 2.

Alternatively, if no more than one photon attains the photo-cathode per beta particle, the number of pulses per second for a given beta source is proportional to the global efficiency of the light measuring system. This allows detection and correction for possible shift.

Theoretical prediction is not straightforward. Roughly, the calculation for the blue screen is as follows.

The mean energy value for beta particles from ^{14}C is 49 KeV. The efficiency of the blue emitting plastic being around 2%, we get, for one beta particle of 49 KeV, 980 eV transmitted to photons in the screen. The maximum emission wavelength is ≈ 420 nm, corresponding to an energy of 3 eV. This leads to 327 photons that are emitted in 4Π. As far as the photo-cathode is seen trough a solid angle of 0.1, 2.6 photons reach this cathode. The quantum efficiency of the cathode is around 0.2, thus we finally get 0.5 photo-electron produced at the cathode for one beta particle. At a first glance, this means that we get a proportionality (factor 0.5) between beta activity and counting rate.

Since the efficiency of the PM tube is significantly less for the red light than for the blue one, one can assume that, when the proportionality is verified for the blue emission, it is also for the red one.

Fulfilling the above conditions can be checked experimentally. One technique consists in observing the pulses using an oscilloscope: they must have the same height whatever the visible surface of the scintillating screen. This surface can be modified by use of a mask. Another technique consists in verifying the linearity of the counting by use of well-known attenuation filters. The counting-rate should match exactly the attenuation factor of the filters

In the present work, the radiocarbon source was obtained by evaporating a commercial solution doped with radiocarbon mixed to cellulose-acetate dissolved in acetone onto the bottom of the disk supporting the screen. However, it can be better to use a commercially available "planchet source". This avoids manipulation of radiocarbon and guarantees a better homogeneity of the surface activity. The total activity of the radiocarbon source was around 200 kBq.

Counting results

Table 1 shows the counting results that were obtained, using a bi-alkali 9635 QA EMI PM-tube, fitted with a "blue" band-pass filter Shott BG12 (maximum transmission at around 400nm) and a "red" high-pass sharp-cut filter Shott 610FG (50% transmission at around 600 nm).

Light source	Filter	
	BG 12 (blue)	610FG (red)
red	1200	255
blue	2800	28
none (= dark counts)	22	22

Table 1.
Counting results in counts/s.

It can be observed that the "red" source has a significant blue component. With these figures, a counting time of 100s allows a standard deviation of less than 1% with the red source. This is enough for most luminescence experiments.

Aknowledgements

Authors would like to acknowledge valuable help from Christophe Dujardin, LPCML, Université Claude Bernard, Lyon, who provided LuAg and related information.

References

Hashimoto, T., Yokosaka K. and Habuki H., (1987) Emission properties of thermoluminescence from natural quartz : blue and red response to absorbed dose. Nucl. Tracks Radiat. Meas. **13**, 57-66.

Obituary

John C. Alldred 1941-2002

John Alldred died in March this year aged 61, shortly after being diagnosed with lung cancer (not unexpected to those of us who knew him as a chain smoker).

John was at the Research Laboratory for Archaeology at 6 Keble Road, Oxford when I arrived there in 1969. He was employed as a research engineer and was responsible for electronic developments, principally for the thermoluminescence group. Particularly in those days, success in research was highly dependent upon a laboratory's expertise in equipment development, appropriate commercial products not usually being available. A critical advance in utilizing the generally low levels of thermoluminescence involved in the dating of pottery was development by John of the photon counting system now widely used in luminescence studies; this was presented at the Second International Conference on Luminescence Dosimetry held in Gatlinburg, Tennessee in 1968. Among his other developments was the fluxgate gradiometer, the forerunner of one of the two types of equipment presently used in the magnetic location of buried remains.

John had studied Physics at Brasenose College, Oxford (subsequently completing an M.Phil.) and this enabled him to be much more than an electronic boffin; he was patient with the electronically ignorant and he gave freely of his time to other researchers. He was a valued member of a number of fieldwork expeditions. His publications include one which became a basic reference paper in luminescence dating:- Aitken, M.J. and Alldred, J.C. (1972) The assessment of error limits in thermoluminescent dating. Archaeometry, 14, 257-267.

After a number of years in the Research Laboratory for Archaeology, John joined Protovale Oxford Ltd, designers and manufacturers of Industrial Metal Detectors and Instruments for Non-destructive Testing in Civil Engineering. He was also well known as a writer of a web site that helped people create their own web sites. At a personal level, he was self-effacing, quietly supportive of those around him; outside the laboratory he helped many people who, like him, had an addiction to alcohol. In his case, he gained an extra 23 years by giving it up completely. Fortunately, his other great love, Indian Cuisine, was indulged in every night without affecting his health.

Ann Wintle

Bibliography

(from 1st April 2002 to 30th September 2002) Compiled by Ann Wintle

---

Amit R., Zilberman E., Enzel Y., and Porat N. (2002) Paleoseismic evidence for time dependency of seismic response on a fault system in the southern Arava Valley, Dead Sea rift, Israel. *Geological Society of America Bulletin* **114**, 192-206.

Barreto A. M. F., Bezerra F. H. R., Sugio K., Tatumi S. H., Yee M., Paiva R. P., and Munita C. S. (2002) Late Pleistocene marine terrace deposits in northeastern Brazil: sea-level change and tectonic implications. *Palaeogeography, Palaeoclimatology, Palaeoecology* **179**, 57-69.

Benny P. G. and Bhatt B. C. (2002) High-level gamma dosimetry using phototransferred thermoluminescence in quartz. *Applied Radiation and Isotopes* **56**, 891-894.

Benny P. G., Gundu Rao T. K., and Bhatt B. C. (2002) The E"1'-centre and its role in TL sensitization in quartz. *Radiation Measurements* **35**, 369-373.

Benoit P. H., Akridge G. A., Ninagawa K., and Sears D. W. G. (2002) Thermoluminescence sensitivity and thermal history of type 3 ordinary chondrites: eleven new type 3.0-3.1 chondrites and possible explanations for differences among H, L, and LL chondrites. *Meteoritics and Planetary Science* **37**, 793-805.

Berger G. W., Pillans B. J., Bruce J. G., and McIntosh P. D. (2002) Luminescence chronology of loess-paleosol sequences from southern South Island, New Zealand. *Quaternary Science Reviews* **21**, 1899-1913.

Bray H. E., Bailey R. M., and Stokes S. (2002) Quantification of cross-irradiation and cross-illumination using a Risø TL/OSL DA-15 reader. *Radiation Measurements* **35**, 275-280.

Brooks R. J., Finch A. A., Hole D. E., Townsend P. D., and Wu Z. L. (2002) The red to near-infrared luminescence in alkali feldspar. *Contributions to Mineralogy and Petrology* **143**, 484-494.

Chung H. W., Delincee H., and Kwon J. H. (2002) The application of different detection methods for irradiated dried anchovy and shrimp. *Radiation Physics and Chemistry* **63**, 411-414.

El-Asmar H. M. (2002) Holocene palaeoshorelines along the Manzala lagoon, northeast of the Nile Delta, Egypt. *Neues Jahrbuch fur Geologie und Palaontologie - Monatshefte* **6**, 337-361.

Feathers J. K. (2002) Luminescence dating in less than ideal conditions: case studies from Klasies River main site and Duinefontein, South Africa. *Journal of Archaeological Science* **29**, 177-194.

Ferko T. E., Wang M. S., Hillegonds D. J., Lipscutcz M. E., Hutchison R., Franke L., Scherer P., Schultz L., Benoit P. H., Sears D. W. G., Singhvi A. K., and Bhandari N. (2002) The irradiation history of the Ghubara (L5) regolith breccia. *Meteoritics and Planetary Science* **37**, 311-327.

Forman S. L. and Pierson J. (2002) Late Pleistocene luminescence chronology of loess deposition in the Missouri and Mississippi river valleys, United States. *Palaeogeography, Palaeoclimatology, Palaeoecology* **186**, 25-46.

Frechen M. and van den Berg M. W. (2002) The coversands and timing of Late Quaternary earthquake events along the Peel Boundary Fault in the Netherlands. *Geologie en Mijnbouw* **81**, 61-70.

Frederick C. D., Bateman M. D., and Rogers R. (2002) Evidence for eolian deposition in the sandy uplands of East Texas and the implications for archaeological site integrity. *Geoarchaeology* **17**, 191-217.

Greilich S., Glasmacher U. A., and Wagner G. A. (2002) Spatially resolved detection of luminescence - a unique tool for archaeochronometry. *Naturwissenschaften* **89**, 371-375.

Grün R. and Ward K. (2002) A long-term fading study for ESR intensity measurement and dose evaluation on fossil tooth enamel. *Radiation Measurements* **35**, 269-274.

Hashimoto T., Nakagawa T., Hong D. G., and Takano M. (2002) An automated system for both red/blue thermoluminescence and optically stimulated luminescence measurement. *Journal of Nuclear Science and Technology* **39**, 108-109.

Hashimoto T., Nakagawa T., Usuda H., and Yawata T. (2002) Development of an automated system equipped with a small X-ray irradiator for red/blue thermoluminescence and optically stimulated luminescence measurement from natural minerals (in Japanese). *Bunseki Kagaku* **51**, 625-632.

Hashimoto T., Yanagawa Y., and Yamaguchi T. (2002) Infrared microspectrometric characterizations and thermoluminescencent properties for natural quartz slices. *Bunseki Kagaku* **51**, 527-532.

Hatte C., Pessenda L. C., Lang A., and Paterne M. (2001) Development of accurate and reliable C-14 chronologies for loess deposits: application to the loess sequence of Nussloch (Rhine Valley, Germany). *Radiocarbon* **43**, 611-618.

Holdaway R. N., Roberts R. G., Beavan-Athfield N. R., Olley J. M., and Worthy T. H. (2002) Optical dating of quartz sediments and accelerator mass spectrometry 14C dating of bone gelatin and moa eggshell: a comparison of age estimates for non-archaeological deposits in New Zealand. *Journal of the Royal Society of New Zealand* **32**, 463-505.

Hossain S. M., de Corte F., Vandenberghe D., and van den Haute P. (2002) A comparison of methods for the annual radiation dose determination in the luminescence dating of loess sediment. *Nuclear Instruments and methods A* **490**, 598-613.

Kaufman D. S., Forman S. L., and Bright J. (2001) Age of the Cutler Dam Alloformation (Late Pleistocene), Bonneville Basin, Utah. *Quaternary Research* **56**, 322-334.

Khan H. M., Bhatti I. A., and Delincee H. (2002) Thermoluminescence of contaminating minerals for the detection of radiation treatment of dried fruits. *Radiation Physics and Chemistry* **63**, 403-406.

Kovacs A., Baranyai M., Wojnarovits L., Miller S., Murphy M., McLaughlin W. L., Slezsak I., and Kovacs A. I. (2002) Applicability of the Sunna dosimeter for food irradiation control. *Radiation Physics and Chemistry* **63**, 777-780.

Kwon J. H., Jeong J., and Chung H. W. (2002) Thermoluminescence characteristics of minerals from irradiated potatoes of different origins of production. *Radiation Physics and Chemistry* **63**, 415-418.

Laruhin M. A., van Es H. J., Bulka G. R., Turkin A. A., Vainshtein D. I., and den Hartog H. W. (2002) EPR study of radiation-induced defects in the thermoluminescence dating medium zircon (ZrSiO4). *Journal of Physics - Condensed Matter* **14**, 3813-3831.

Lawless J. M., Lam S. K., and Lo D. (2002) Non-destructive in situ thermoluminescence using CO2 laser heating. *Optica Express* **10**, 291-296.

Lawson M. P. and Thomas D. S. G. (2002) Late Quaternary lunette dune sedimentation in the southwestern Kalahari desert, South Africa: luminescence based chronologies of aeolian activity. *Quaternary Science Reviews* **21**, 825-836.

Li S. H. (2002) Luminescence sensitivity changes of quartz by bleaching, annealing and UV exposure. *Radiation Effects and Defects in Solids* **157**, 357-364.

Li S. H., Sun J. M., and Zhao H. (2002) Optical dating of dune sands in the northeastern deserts of China. *Palaeogeography, Palaeoclimatology, Palaeoecology* **181**, 419-429.

Lian L. B. and Huntley D. J. (2001) Luminescence dating. In *Tracking Environmental Change Using Lake Sediments*, Vol. 1 (ed. W. M. L. a. J. P. Smol), pp. 261-282. Kluwer Academic Publishers.

Little E. C., Lian O. B., Velichko A. A., Morozova T. D., Nechaev V. P., Dlussky K. G., and Rutter N. W. (2002) Quaternary stratigraphy and optical dating of loess from the east European Plain (Russia). *Quaternary Science Reviews* **21**, 1745-1762.

Lu Y. C., Prescott J. R., Zhao H., Chen J., and Wei L. Y. (2002) Optical dating of colluvial deposits from Xiyangfang, China, and the relation to palaeo-earthquake events. *Quaternary Science Reviews* **21**, 1087-1097.

Mangerud J., Astakhov V., and Svendsen J. I. (2002) The extent of the Barents-Kara Ice Sheet during the Last Glacial Maximum. *Quaternary Science Reviews* **21**, 111-119.

Mayer J. H. (2002) Evaluating natural site formation processes in eolian dune sands: a case study from the Krmpotich Folsom site, Killpecker Dunes, Wyoming. *Journal of Archaeological Science* **29**, 1199-1211.

Murray A. S. and Olley J. M. (2002) Precision and accuracy in the optically stimulated luminescence dating of sedimentary quartz: a status review. *Geochronometria* **21**, 1-16.

Murray-Wallace C. V., Banerjee D., Bourman R. P., Olley J. M., and Brooke B. P. (2002) Optically stimulated luminescence dating of Holocene relict foredunes, Guichen Bay, South Australia. *Quaternary Science Reviews* **21**, 1077-1086.

Murray-Wallace C. V., Jones B. G., Nghi T., Price D. M., Van Vinh V., Tinh T. N., and Nanson G. C. (2002) Thermoluminescence ages for a reworked coastal barrier, southeastern Vietnam: a preliminary report. *Journal of Asian Earth Sciences* **20**, 535-548.

Nichol S. L. (2002) Morphology, stratigraphy and origin of last interglacial beach ridges at Bream Bay, New Zealand. *Journal of Coastal Research* **18**, 149-159.

Nott J., Price D., and Nanson G. (2002) Stream response to Quaternary climate change: evidence from the Shoalhaven River catchment, southeastern highlands, temperate Australia. *Quaternary Science Reviews* **21**, 965-974.

Novothny A., Horvath E., and Frechen M. (2002) The loess profile of Albertirsna, Hungary - improvements in loess stratigraphy by luminescence dating. *Quaternary International* **95-96**, 155-163.

Pledge N. S., Prescott J. R., and Hutton J. T. (2002) A late Pleistocene occurrence of Diprotodon at Hallett Cove, South Australia. *Transactions of the Royal Society of South Australia* **126**, 39-44.

Poolton N. R. J., Ozanyan K. B., Wallinga J., Murray A. S., and Bøtter-Jensen L. (2002) Electrons in feldspar II: a consideration of the influence of conduction band-tail states on luminescence processes. *Physics and Chemistry of Minerals* **29**, 217-225.

Poolton N. R. J., Wallinga J., Murray A. S., and Bøtter-Jensen L. (2002) Electrons in feldspar I: on the wavefunction of electrons trapped at simple lattice defects. *Physics and Chemistry of Minerals* **29**, 210-216.

Pope R. J. J. and Millington A. C. (2002) The role of alluvial fans in mountainous and lowland drainage systems: examples from the Sparta Basin, Lakonia, southern Greece. *Zeitschrift fur Geomorphologie* **46**, 109-136.

Porat N., Chazan M., Schwarcz H., and Horwitz L. K. (2002) Timing of the Lower to Middle Paleolithic boundary: new dates from the Levant. *Journal of Human Evolution* **43**, 107-122.

Prescott J. R., Robertson G. B., and Williams F. M. (2002) Luminescence ages beyond 500 ka: can they be believed? In *Australian Connections and New Directions* (ed. M. Jones and P. Sheppard), pp. 271-284.

Preusser F., Radies D., and Matter A. (2002) A 160,000-year record of dune development and atmospheric circulation in southern Arabia. *Science* **296**, 2018-2020.

Rasmussen K. L. (2001) Provenance of ceramics revealed by magnetic susceptibility and thermoluminescence. *Journal of Archaeological Science* **28**, 451-456.

Richter D., Schroeder H. B., Rink W. J., Julig P. J., and Schwarcz H. P. (2001) The Middle to Upper Palaeolithic transition in the Levant and new thermoluminescence dates for a Late Mousterian assemblage from Jerf al-Ajla Cave (Syria). *Paléorient* **27/2**, 29-46.

Ringrose S., Kampunzu A. B., Vink B. W., Matheson W., and Downey W. S. (2002) Origin and palae-environments of calcareous sediments in the Moshawengdry valley, southeast Botswana. *Earth Surface Processes and Landforms* **27**, 591-611.

Rink W. J., Karavanic I., Pettitt P. B., van der Plicht J., Smith F. H., and Bartoll J. (2002) ESR and AMS-based 14C dating of Mousterian levels at Mujina Pecina, Dalmatia, Croatia. *Journal of Archaeological Science* **29**, 943-952.

Rousseau D. D., Antoine P., Hatté C., Lang A., Zöller L., Fontugne M., Ben Othman D., Luck J. M., Moine O., Labonne M., Bentaleb I., and Jolly D. (2002) Abrupt millennial climatic changes from Nussloch (Germany) Upper Weichselian eolian records during the Last Glaciation. *Quaternary Science Reviews* **21**, 1577-1582.

Ruffini R., Borghi A., Cossio R., Olmi F., and Vaggelli G. (2002) Volcanic quartz growth zoning identified by cathodoluminescence and EPMA studies. *Mikrochimica Acta* **139**, 151-158.

Sato H., Takatsuji T., Takada J., Endo S., Hoshi M., Sharofov V. F., Veselkina I. I., Pilenko I. V., Kalimullin W. A. F., Masyakin V. B., Yoshikawa I., Nagatomo T., and
Okajima S. (2002) Measuring the external exposure dose in the contaminated area near the Chernobyl nuclear power station using the thermoluminescence of quartz in bricks. *Health Physics* **83**, 227-236.

Schwamborn G., Rachold V., and Grigoriev M. N. (2002) Late Quaternary sedimentation history of the Lena Delta. *Quaternary International* **89**, 119-134.

Shane P., Lian O. B., Augustinus P., Chisari R., and Heijnis H. (2002) Tephrostratigraphy and geochronology of a ca. 120 ka terrestrial record at Lake Poukawa, North Island, New Zealand. *Global and Planetary Change* **33**, 221-224.

Shaw A., Holmes P., and Rogers J. (2002) Depositional landforms and environmental change in the headward vicinity of Dias Beach, Cape Point. *South African Journal of Geology* **104**, 101-114.

Souza D. N., de Lima J. F., Valerio M. R. G., Fantini C., Pimenta M. A., Moreira R. I., and Caldas L. V. E. (2002) Influence of thermal treatment on the Raman, infrared and TL responses of natural topaz. *Nuclear Instruments and Methods B* **191**, 230-235.

Souza D. N., Lima J. F., Valerio M. E. G., Alves E., and Caldas L. V. E. (2002) Effects of ion implantation on the thermoluminescent properties of natural colourless topaz. *Nuclear Instruments and Methods B* **191**, 196-201.

Souza S. O., Chubaci J. F. D., Selvin P. C., Sastry M. D., and Watanabe S. (2002) Thermoluminescence and EPR studies on natural petalite crystals. *Journal of Physics D- Applied Physics* **35**, 1562-1565.

Suresh N., Bagati T. N., Thakur V. C., Kumar R., and Sangode S. J. (2002) Optically stimulated luminescence dating of alluvial fan deposits of Pinjaur Dun, NW Sub Himalaya. *Current Science* **82**, 1267-1274.

Tanir G., Okuducu S., and Gulen S. (2002) The dependence of OSL intensity on radiation dose for samples of chlorides contained in feldspars. *Czechoslovak Journal of Physics* **52**, 963-968.

Thomas D. S. G. and Shaw P. A. (2002) Late Quaternary environmental change in central southern Africa: new data, synthesis, issue and prospects. *Quaternary Science Reviews* **21**, 783-797.

Turkin A. A., van Es H. J., Vainshtein D. I., and den Hartog H. W. (2002) A kinetic model of zircon thermoluminescence. *Nuclear Instruments and Methods B* **191**, 37-43.

Ufimtsev G. F., Shibanova I. V., Kulagina N. V., Mascik I. M., Perevalov A. V., Rezanova A. V., Vogt T., Ignatova N. V., and Misharina V. A. (2002) Upper Pleistocene to Holocene deposits of the Tunka rift (southern Baikal region). *Stratigraphy and Geological Correlation* **10**, 295-304.

van Es H. J., Vainshtein D. I., Rozendaal A., Donoghue J. F., de Meijer R. J., and den Hartog H. W. (2002) Thermoluminescence of ZrSiO4 (zircon): a new dating method? *Nuclear Instruments and Methods B* **191**, 649-652.

van Huissteden K., Schwan J. C. G., and Bateman M. D. (2001) Environmental conditions and paleowind directions at the end of the Weichselian Late Pleniglacial recorded in aeolian sediments and geomorphology (Twente, Eastern Netherlands). *Geologie en Mijnbouw* **80**, 1-18.

Vora K. H., Gaur A. S., Price D., and Sundaresh. (2002) Cultural sequence of Bet Dwarka island based on thermoluminescence dating. *Current Science* **82**, 1351-1356.

Wallinga J. (2002) On the detection of OSL age overestimation using single-aliquot techniques. *Geochronometria* **21**, 17-26.

Wegmuller S., Preusser F., Muller B. U., and Schluchter C. (2002) Palynostratigraphic investigation and luminescence dating of the Galgenmoos section and implications for the chronology of the last glacial cycle in the northern Alpine Foreland of Switzerland (in German). *Ecologae Geologicae Helvetiae* **95**, 115-126.

Whitley V. H. and McKeever S. W. S. (2000) Photoionization of deep centers in Al2O3. *Journal of Applied Physics* **87**, 249-256.

Wood W. W., Stokes S., and Rich J. (2002) Implications of water supply for indigenous Americans during Holocene aridity phases on the Southern High Plains. *Quaternary Research* **58**, 139-148.

Xiong S., Ding Z., Liu T., and Zhang J. (2002) East Asian monsoon instability at the stage 5a/4 transition. *Boreas* **31**, 126-132.

Yasuda H., Kobayashi I., and Morishima H. (2002) Decaying patterns of optically stimulated luminescence from Al2O3:C for different quality radiations. *Journal of Nuclear Science and Technology* **39**, 211-213.

Yim W. W.-S., Price D. M., and Choy A. M. S. F. (2002) Distribution of moisture contents and thermoluminescence ages in an inner shelf borehole from the new Hong Kong International airport site, China. *Quaternary International* **92**, 35-43.

Yoshimura E. M., Okuno E., and Suszynska M. (2002) Gamma irradiated soda lime silicate glasses of different origin: isothermal light emission. *Nuclear Instruments and Methods B* **191**, 375-378.

Young R. W., Young A. R. M., Price D. M., and Wray R. A. L. (2002) Geomorphology of the Namoi alluvial plain, northwestern New South Wales. *Australian Journal of Earth Sciences* **49**, 509-523.

Selected papers from Radiation Protection Dosimetry, v 100 and 101

Proceedings of the Solid State Dosimetry Conference in Athens, 2001
Complete listing of papers available on http://www.ntp.org.uk/rpd/rpdind.html

Bailey R. (2002) Simulations of variability in the luminescence characteristics of natural quartz and its implications for estimates of absorbed dose. *Radiation Protection Dosimetry* **100**, 33-38.

Bailiff I. K., Correcher V., Delgado A., Göksu Y., and Hübner S. (2002) Luminescence characteristics of dental ceramics for retrospective dosimetry - a preliminary study. *Radiation Protection Dosimetry* **101**, 519-524.

Banerjee D., Blair M., Lepper K., and McKeever S. W. S. (2002) Optically stimulated luminescence signals of polymineral fine-grains in the JSC Mars-1 soil simulant sample. *Radiation Protection Dosimetry* **101**, 321-326.

Banerjee D., Blair M., and McKeever S. W. S. (2002) Dose and dose-rate dependence of optically stimulated signals in quartz: theoretical simulations. *Radiation Protection Dosimetry* **101**, 353-358.

Banerjee D., Page K., and Lepper K. (2002) Optical dating of paleochannel deposits in the Riverine Plain, Southeastern Australia: testing the reliability of existing thermoluminescence dates. *Radiation Protection Dosimetry* **101**, 327-332.

Berger T., Hajek M., Primerano W., and Vana N. (2002) Thermoluminescence dating of archaeological artefacts from the middle Neolithic, Bronze Age and the Roman Empire period. *Radiation Protection Dosimetry* **101**, 363-366.

Bos A. J. J., Winkelman A. J. M., Le Masson N. J. M., Sidorenko A. V., and van Eijk C. W. E. (2002) A TL/OSL emission spectrometer extension of the Risø Reader. *Radiation Protection Dosimetry* **101**, 111-114.

Bøtter-Jensen L. and Murray A. S. (2002) Optically stimulated luminescence in retrospective dosimetry. *Radiation Protection Dosimetry* **101**, 309-314.

Bøtter-Jensen L., Bulur E., Murray A. S., and Poolton N. R. J. (2002) Enhancements in luminescence measurement techniques. *Radiation Protection Dosimetry* **101**, 119-124.

Chen R. (2002) The role of retrapping in dose dependence of pulsed optically stimulated luminescence. *Radiation Protection Dosimetry* **100**, 71-74.

Chithambo M. L. (2002) Time-resolved luminescence from annealed quartz. *Radiation Protection Dosimetry* **100**, 273-276.

Gomez-Ros J. M., Correcher V., Garcia-Guinea J., and Delgado A. (2002) Kinetic parameters of lithium and aluminium doped quartz from thermoluminescence glow curves. *Radiation Protection Dosimetry* **100**, 399-402.

Haustein M. and Krbetschek M. R. (2002) Red thermoluminescence of quartz and its application in dating archaeometallurgical slag. *Radiation Protection Dosimetry* **101**, 375-378.

Hoffmann D. and Mangini A. (2002) Comparative studies on the CO2 signal in tooth enamel and carbonates. *Radiation Protection Dosimetry* **101**, 359-362.

Jain M., Bøtter-Jensen L., Murray A. S., and Jungner H. (2002) Retrospective dosimetry: dose evaluation using unheated and heated quartz from a radioactive waste storage building. *Radiation Protection Dosimetry* **101**, 525-530.

Kitis G., Pagonis V., Carty H., and Tatsis E. (2002) Detailed kinetic study of the thermoluminescence glow curve of synthetic quartz. *Radiation Protection Dosimetry* **100**, 225-228.

Lepper K. and McKeever S. W. S. (2002) An objective methodology for dose distribution analysis. *Radiation Protection Dosimetry* **101**, 349-352.

Murray A. S. and Wintle A. G. (2002) Retrospective dose assessment: the measurement of dose in quartz in dating and accident dosimetry. *Radiation Protection Dosimetry* **101**, 301-308.

Murray A. S., Wintle A. G., and Wallinga J. (2002) Dose estimation using quartz OSL in the non-linear region of the growth curve. *Radiation Protection Dosimetry* **101**, 371-374.

Nanjundaswamy R., Lepper K., and McKeever S. W. S. (2002) Thermal quenching of thermoluminescence in natural quartz. *Radiation Protection Dosimetry* **100**, 305-308.

Pagonis V., Tatsis E., Kitis G., and Drupieski C. (2002) Search for common characteristics in the glow-curves of quartz of various origins. *Radiation Protection Dosimetry* **100**, 373-376.

Thomsen K., Bøtter-Jensen L., and Murray A. S. (2002) Household and workplace chemicals as retrospective luminescence dosemeters. *Radiation Protection Dosimetry* **101**, 515-518.

Thomsen, K., Bøtter-Jensen L., Murray A. S., and Solongo S. (2002) Retrospective dosimetry using unheated quartz: a feasibility study. *Radiation Protection Dosimetry* **101**, 345-348.

Townsend P. D., Parish R., and Rowlands A. P. (2002) A new interpretation of depth-age profiles. *Radiation Protection Dosimetry* **101**, 315-320.

Visocekas R. (2002) Tunnelling in afterglow: its coexistence and interweaving with thermally stimulated luminescence. *Radiation Protection Dosimetry* **100**, 45-54.

Wallinga J., Murray A. S., and Bøtter-Jensen L. (2002) Measurement of the dose in quartz in the presence of feldspar contamination. *Radiation Protection Dosimetry* **101**, 367-370.

Wallinga J., Murray A. S., Wintle A. G., and Bøtter-Jensen L. (2-002) Electron-trapping probability in natural dosemeters as a function of irradiation temperature. *Radiation Protection Dosimetry* **101**, 339-344.

Woda C., Schilles T., Rieser U., Mangini A., and Wagner G. A. (2002) Point defects and the blue emission in fired quartz at high doses: a comparative luminescence and ESR study. *Radiation Protection Dosimetry* **100**, 261-264.

Zacharias N., Mauz B., and Michael C. T. (2002) Luminescence quartz dating of lime mortars: a first approach. *Radiation Protection Dosimetry* **101**, 379-382.

Zhao H. and Li S. H. (2002) Luminescence isochron dating: a new approach using different grain sizes. *Radiation Protection Dosimetry* **101**, 333-338.